Chapter 4

Nonclassical properties of coupled cavity OMS

4.1 Introduction

In previous chapter, we have studied OMS with single cavity and interaction between two field modes (photon and phonon). Here, we pay our attention on two cavity system, where the cavities are coupled by photon hopping interaction. The system has multiple field modes. So, there is a possibility of different types of multimode nonclassical correlation. Nonclassical correlation for multi field modes have already been examined and reported to different optical systems such as coherent transport without transit [151], four-wave mixing process in optical lattice [152, 153], molecular dissociation [154], Bose-Hubbard chains [155] etc. Multimode nonclassicalities have potential application frequency comb via atomic system [156], non-demolishing measurement [157], quantum metrology [158], multiplexed microscopic memories [159] etc.

Two cavity OMS has been studied via three and four field modes to address different important optomechanical aspects. For example, nonlinearities in single photon optomechanics [160], transfer of entangled state [161], mechanical squeezing at resolved sideband regime [162], coherent absorption, amplification and transmission [163] etc. In present chapter, we have analyzed rigorously three types of nonclassicalities both for single and compound field mode, in two cavity OMS. Study of entanglement has been done so far in this type of system in reference [164, 165]. In both reference there is an analysis of entangled state generation between two macroscopic resonators. These studies are confined only to non-separability between two mechanical modes. Here, we have extensively investigated nonclassical correlations in lower as well as higher order field modes. We have also addressed the possible regime of photon tunnelling and coupling strength where nonclassicalities exists.

4.2 System Description

We consider a two cavity system, each cavity having a fixed mirror and a movable mirror [164] (Figure 4.1). The cavity field is integrated with the small amplitude mechanical motion via radiation pressure interaction. To fulfill this type of interaction at quantum regime, the mechanical system is required to cool sufficiently. The two cavity field modes are coupled via photon-hopping interaction. The total Hamiltonian of the model system is given by

$$H = \sum_{k=1,2} [\omega_c\, a_k^\dagger a_k \; + \omega_m b_k^\dagger b_k \; - g a_k^\dagger a_k \; (b_k^\dagger + b_k \,)] - \xi (a_1^\dagger a_2 \; + a_2^\dagger a_1 \,) \qquad (4.1)$$

The part of the Hamiltonian under the summation corresponds to each cavity system with optomechanical interaction. The annihilation (creation) operator a_k $(a_k^\dagger)$ and b_k $(b_k^\dagger)$ correspond to cavity field mode and mechanical mode, respectively.

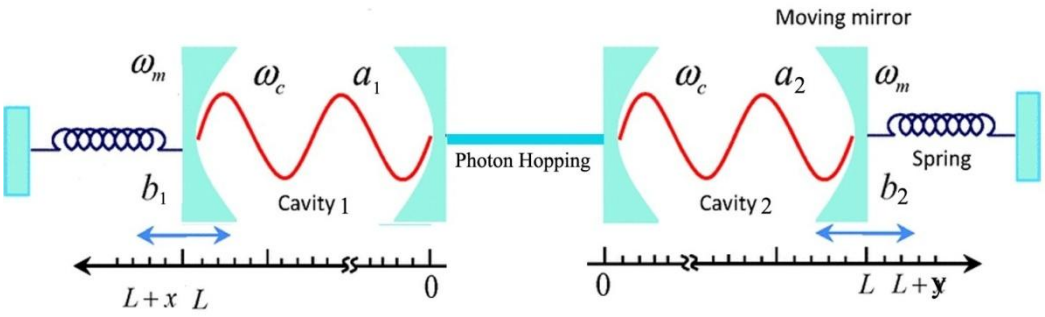

Figure 4.1: Schematic depiction of two cavity system coupled via photon hopping. Each cavity system consists with a fixed mirror and a movable mirror.

The cavity resonance frequency is $\omega_c = 2\pi c/l$; where l is the length of the cavity. Due to radiation pressure, x and y are the displacement of the moving mirrors in cavity 1 and cavity 2, respectively. The corresponding frequencies are given by the relation $\omega_c(1) = 2\pi c/(l + x)$ and $\omega_c(2) = 2\pi c/(l + y)$. Here, we assume both the

displacements are very small as compared to length of the cavities ($x\ and\ y \ll l$). ω_m represents the frequency of mechanical moving system undergo small amplitude oscillations. The intra-cavity strength of coupling between cavity mode and mechanical mode is given by g. The part without summation corresponds to interaction between two cavity fields via photon hopping interaction strength ξ.

4.3 Quantum Dynamics

Heisenberg EOM corresponds to cavity field modes and mechanical modes are as follows:

$$\frac{da_k}{dt} = -i\left[\omega_c a_k(t) - g\{a_k(t)b_k^\dagger(t) + a_k(t)b_k(t)\} - \xi\, a_j(t)\right]$$

$$\frac{db_k}{dt} = -i[\omega_m b_k(t) - g a_k^\dagger(t) a_k(t)] \tag{4.2}$$

where $k, j = 1,2$ and $k \neq j$.

The solutions of equations (4.2) in-terms of time dependent coefficients ($A_i's\ and\ B_i's$) are

$$\begin{aligned} a_k(t) = {} & A_1 a_k(0) + A_2 a_k(0) b_k^\dagger(0) + A_3 a_k(0) b_k(0) + A_4 a_j(0) + A_5 a_k(0) b_k^{\dagger 2}(0) \\ & + A_6 a_k(0) + A_7 a_k(0) b_k^\dagger(0) b_k(0) + A_8 a_k(0) b_k^2(0) + A_9 a_k^\dagger(0) a_k^2(0) \\ & + A_{10} a_j(0) b_k^\dagger(0) + A_{11} a_j(0) b_j^\dagger(0) + A_{12} a_j(0) b_j(0) \\ & + A_{13} a_j(0) b_k(0) + A_{14} a_k(0) \end{aligned}$$

$$b_k(t) = B_1 b_k(0) + B_2 a_k^\dagger(0)\, a_k(0) + B_3 a_k^\dagger(0) a_j(0) + B_4 a_j^\dagger(0) a_k(0) \tag{4.3}$$

The time dependent coefficients have been analyzed from the initial boundary condition $A_1(0) = B_1(0) = 1$ and $A_i(0) = 0$ for $i = 2, \ldots, 14$ and $B_i(0) = 0$ for $i = 2, \ldots, 4$ (related differential equations are in appendix B). The expressions of the coefficients are as follows:

$$A_1 = e^{-i\omega_c t}$$

$$A_2 = \frac{g}{\omega_m} A_1(F(t) - 1)$$

$$A_3 = \frac{g}{\omega_m} A_1(1 - F^*(t))$$

$$A_4 = i\xi t A_1$$

$$A_5 = \frac{g^2}{2\omega_m^2} A_1(F(t) - 1)^2$$

$$A_6 = \frac{g^2}{\omega_m^2} A_1\{(F^*(t) - 1) + i\omega_m t\}$$

$$A_7 = \frac{g^2}{\omega_m^2} A_1\{F^*(t) + F(t) - 2\}$$

$$A_8 = \frac{g^2}{2\omega_m^2} A_1(F^*(t) - 1)^2$$

$$A_9 = \frac{g^2}{2\omega_m^2} A_1\{F^*(t) - F(t) + 2i\omega_m t\}$$

$$A_{10} = \frac{g\xi}{{\omega_m}^2} A_1\{F(t)(i\omega_m t - 1) + 1\}$$

$$A_{11} = \frac{g\xi}{{\omega_m}^2} A_1\{F(t) - (i\omega_m t - 1)\}$$

$$A_{12} = \frac{g\xi}{{\omega_m}^2} A_1\{F^*(t) + (i\omega_m t - 1)\}$$

$$A_{13} = -\frac{g\xi}{{\omega_m}^2} A_1\{F^*(t)(i\omega_m t + 1) - 1\}$$

$$A_{14} = -\frac{\xi^2 t^2}{2} A_1$$

$$B_1 = F^*(t)$$

$$B_2 = \frac{g}{\omega_m} A_1(1 - B_1)$$

$$B_3 = \frac{g\xi}{{\omega_m}^2} A_1\{B_1 + (i\omega_m t - 1)\}$$

$$B_4 = -B_3 \tag{4.4}$$

Where $F(t) = e^{i\omega_m t}$.

In the solution, we neglect the terms beyond quadratic coefficient of the coupling strength and photon hopping interaction parameter. Here, the coefficients A_2, A_3, A_4 and B_2 linearly depend on interaction parameters and A_i $(i = 5, \dots, 14)$, B_3 and B_4 are quadratic function of interaction parameters.

We have used equal time commutation relations, to confirm the validity of the solutions.

$$[a_k(t), a_k{}^{\dagger}(t)] = \left[b_k(t), b_k{}^{\dagger}(t)\right] = 1$$

In ref. [166], Jae et al established that the optical system shows nonclassical effects with coherent input. Considering this, we assume initial state is the product of four coherent states such as $|\psi\rangle = |\alpha_1\rangle \otimes |\alpha_2\rangle \otimes |\beta_1\rangle \otimes |\beta_2\rangle$ where $|\alpha_1\rangle$, $|\alpha_2\rangle$, $|\beta_1\rangle$ and $|\beta_2\rangle$ are the eigenkets of the two cavity field modes and mechanical modes, for operators a_1, a_2, b_1 and b_2 respectively. Thus, $a_1 |\psi\rangle = \alpha_1 |\psi\rangle$.

4.4 Quantum Squeezing

In this section, we illustrate the possibility of single mode squeezing in lower as well as higher order for all the cavity field modes and mechanical modes. The intermodal squeezing between the fields mode are also studied.

4.4.1 Lower order single mode squeezing

Using equation (2.6) and solutions of equation (4.3), we obtain the variances of the field quadratures as follows:

$$\begin{pmatrix}(\Delta X_{a_k})^2\\(\Delta Y_{a_k})^2\end{pmatrix} = \frac{1}{4}[1 + |A_3|^2 + |A_4|^2 + 2|A_2|^2(|\alpha_k|^2 + |\beta_k|^2) + \{A_1^*(A_6 + A_{14} + A_7|\beta_k|^2 + 2A_9|\alpha_k|^2) + c.c.\} \pm \{(A_9A_1 + A_2A_3)\alpha_k{}^2 + c.c.\}] \quad (4.5)$$

$$\begin{pmatrix}(\Delta X_{b_k})^2\\(\Delta Y_{b_k})^2\end{pmatrix} = \frac{1}{4}[1 + 2|B_2|^2|\alpha_k|^2 + (B_2^{*2}|\alpha_k|^2 + c.c.)] \quad (4.6)$$

Equation (4.5) and (4.6) are the variance of quadratures for cavity field and mechanical mode, respectively. From equation (4.6), it is clear that there is a possibility of single mode optical field squeezing. Figure 4.2 displays the temporal variation of the variance of the cavity field mode quadratures. Both the quadratures are greater than zero point fluctuation. This is due to smaller contribution of the fluctuation part $\{(A_9A_1 + A_2A_3)\alpha_k{}^2 + c.c.\}$ in the expression, in comparison with the rest part. From equation (4.6), it is concluded that lower order single mode squeezing of mechanical mode is not possible.

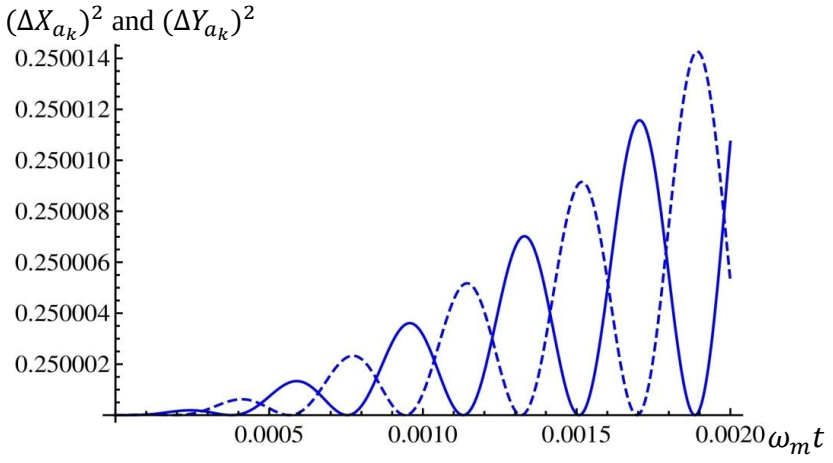

Figure 4.2: Qudrature variation of $(\Delta X_{a_k})^2$ (solid line) and $(\Delta Y_{a_k})^2$ (dashed line) for single cavity field mode with $\omega_m t$ for $|\alpha_k| = 3$, $|\beta_k| = 2$, $g/\omega_m = 0.3$, $g/\xi = 4$, $g = 2\pi \times 0.4$ MHz.

4.4.2 Higher order single mode squeezing

Using the field quadrature operators of $n-th$ single mode squeezing (equation 2.11) and solutions of equation (4.3) we obtain

$$\begin{pmatrix} S_{a_k}(2) \\ Q_{a_k}(2) \end{pmatrix} = A_3^* A_3(1+\mid \alpha_k \mid^2 + 2 \mid {\alpha_k}^2 \mid^2) + (A_1^* A_6 + c.c.) \pm\{(A_1^3 A_9 + A_1^3 A_2 A_3)\alpha_k^4 + c.c.\} \quad (4.7)$$

$$\begin{pmatrix} S_{a_k}(3) \\ Q_{a_k}(3) \end{pmatrix} = 9[A_3^* A_3(2 + 7 \mid \alpha_k \mid^2 + 2 \mid {\alpha_k}^3 \mid^2) + 2A_2^* A_2 \mid \beta_k \mid^2 + (A_1^* A_6 + c.c.)(2 + 3 \mid \alpha_k \mid^2 + \mid \alpha_k^2 \mid^2) \pm \{(A_1^5 A_9 + A_1^4 A_2 A_3)\alpha_k^6 + c.c.\}] \quad (4.8)$$

$$\begin{pmatrix} S_{b_k}(2) \\ Q_{b_k}(2) \end{pmatrix} = 8B_2^* B_2 \mid \alpha_k \mid^2 \mid \beta_k \mid^2 \pm \{2B_1^2 B_2^2(1 - \mid \alpha_k \mid^2) \mid \alpha_k \mid^2 \beta_k^2 + c.c.\} \quad (4.9)$$

Equation (4.7) and (4.8) correspond to the squeezing parameter for amplitude squared and cube quadrature variation of the cavity field mode. Equation (4.9) and (4.10) correspond to amplitude squared and $n-th$ order field quadrature variation of the mechanical mode. Temporal variations of equation (4.7) and (4.8) are shown in figure 4.3 (a-b). From figure (a), it is clear that amplitude squared squeezing is possible for cavity field mode but degree of squeezing is very small. Amplitude cube squeezing is not possible as both the squeezing parameter is positive (shown in figure 4.3 b).

The right side of the equation (4.9) and (4.10) are not simple, so we have plotted these in Fig 4.4 as a function of dimension less parameter $\omega_m t$. The variations show that amplitude squared and fourth order single mode squeezing are possible for the present system. It is interesting to show that one field quadrature is squeezed due to cost of other and the degree of squeezing increases as order grows. The degree of squeezing increases due to presence of the term $n^2 \mid \alpha_k \mid^{2n-4}$ in the expression of equation (4.10). In lower order study in previous section, it is observed that mechanical mode is not

squeezed whereas in higher order study there is a signature of mechanical squeezing. So, this gives the signature of nonclassicalities at macroscopic scale.

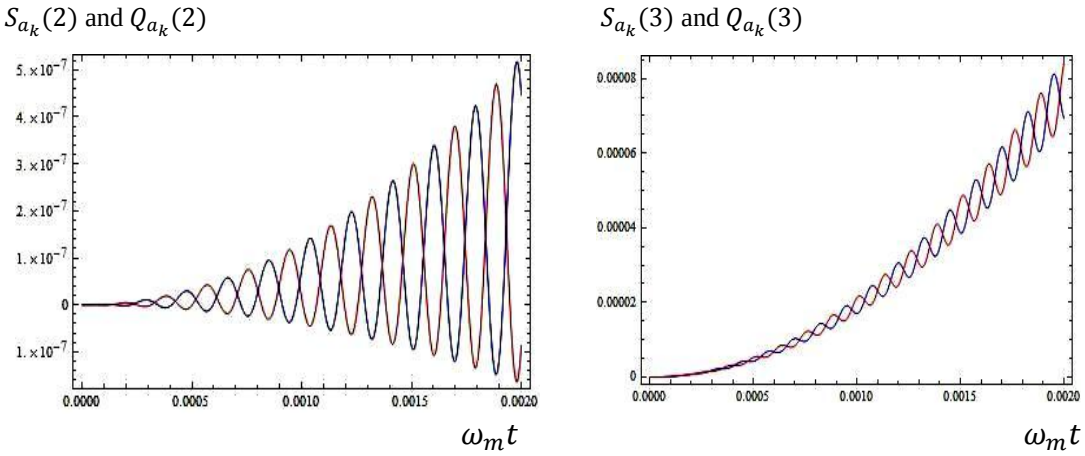

(a) (b)

Figure 4.3: Temporal variation of single cavity field mode squeezing parameters (a) $S_{a_k}(2)$ (blue line) and $Q_{a_k}(2)$ (red line); (b) $S_{a_k}(3)$ (blue line) and $Q_{a_k}(3)$ (red line) for $g/\omega_m = 0.3$, $g/\xi = 4$, $g = 2\pi \times 0.4$ MHz, $|\alpha_k| = 5$, $|\beta_k| = 3$.

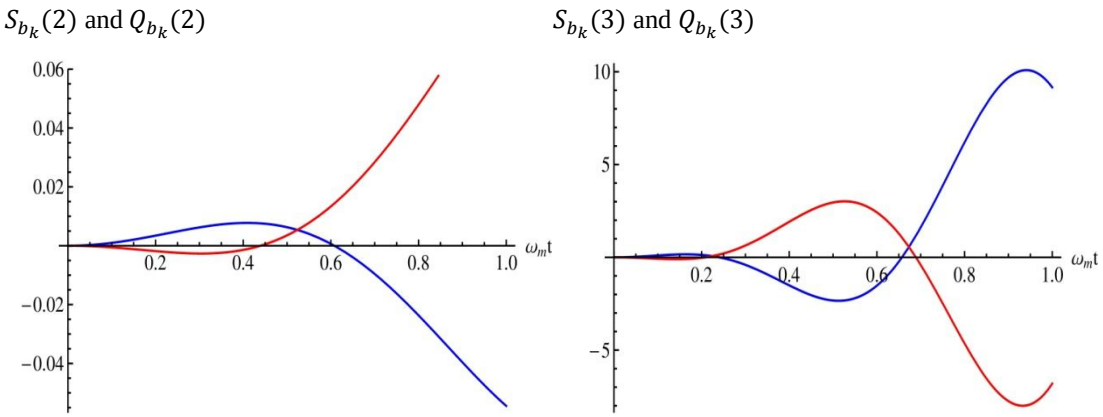

(a) (b)

Figure 4.4: Temporal variation of mechanical field mode squeezing parameters (a) $S_{b_k}(2)$ (blue line) and $Q_{b_k}(2)$ (red line); (b) $S_{b_k}(3)$ (blue line) and $Q_{b_k}(3)$ (red line) for $g/\omega_m = 0.3$, $g/\xi = 4$, $g = 2\pi \times 0.4$ MHz, $|\alpha_k| = 5$, $|\beta_k| = 3$.

4.4.3 Intermodal squeezing

We have derived the analytic expressions of the quadrature variances for different compound mode using equations (2.7, 4.3, 4.5) and (4.6).

$$\begin{pmatrix}(\Delta X_{a_k b_k})^2\\(\Delta Y_{a_k b_k})^2\end{pmatrix} = \frac{1}{2}\left[\begin{pmatrix}(\Delta X_{a_k})^2\\(\Delta Y_{a_k})^2\end{pmatrix} + \begin{pmatrix}(\Delta X_{b_k})^2\\(\Delta Y_{b_k})^2\end{pmatrix}\right]$$

$$\pm\frac{1}{8}\left[\{(A_1B_2 + A_2B_1)\alpha_k + (A_1B_3 + A_{10}B_1)\alpha_j + (A_3B_2 + A_7B_1)\alpha_k\beta_k + (2A_5B_1 + A_2B_2)\alpha_k\beta_k{}^*\} + c.c.\right] \quad (4.11)$$

$$\begin{pmatrix}(\Delta X_{a_k b_j})^2\\(\Delta Y_{a_k b_j})^2\end{pmatrix} = \frac{1}{2}\left[\begin{pmatrix}(\Delta X_{a_k})^2\\(\Delta Y_{a_k})^2\end{pmatrix} + \begin{pmatrix}(\Delta X_{b_j})^2\\(\Delta Y_{b_j})^2\end{pmatrix}\right]$$

$$\pm\frac{1}{8}\{(A_1B_4 + A_4B_2 + A_{11}B_1)\alpha_j + c.c.\} \quad (4.12)$$

$$\begin{pmatrix}(\Delta X_{a_k a_j})^2\\(\Delta Y_{a_k a_j})^2\end{pmatrix} = \frac{1}{2}\left[\begin{pmatrix}(\Delta X_{a_k})^2\\(\Delta Y_{a_k})^2\end{pmatrix} + \begin{pmatrix}(\Delta X_{a_j})^2\\(\Delta Y_{a_j})^2\end{pmatrix}\right] \quad (4.13)$$

$$\begin{pmatrix}(\Delta X_{b_k b_j})^2\\(\Delta Y_{b_k b_j})^2\end{pmatrix} = \frac{1}{2}\left[\begin{pmatrix}(\Delta X_{b_k})^2\\(\Delta Y_{b_k})^2\end{pmatrix} + \begin{pmatrix}(\Delta X_{b_j})^2\\(\Delta Y_{b_j})^2\end{pmatrix}\right] \quad (4.14)$$

From the expressions of equation (4.11, 4.12) and (4.13), it is clear that intermodal squeezing is possible for compound mode $a_k b_k$, $a_k b_j$ and $a_k a_j$. The variation of the expression (4.11) is displayed in figure 4.5 (a). From the expression of fluctuation part of the field quadratures it can be stated that degree of squeezing depends on coupling strength, photon tunneling strength and also on input phase. Keeping photon tunneling strength constant (parametric condition) if we increase coupling strength (few tens MHz), degree of it also increases. Again, keeping coupling strength constant (graphical condition), if we increase photon tunneling strength (few hundred MHz), the degree of squeezing remains same. This is because intra-cavity field modes are affected by coupling strength, not by photon tunneling strength.

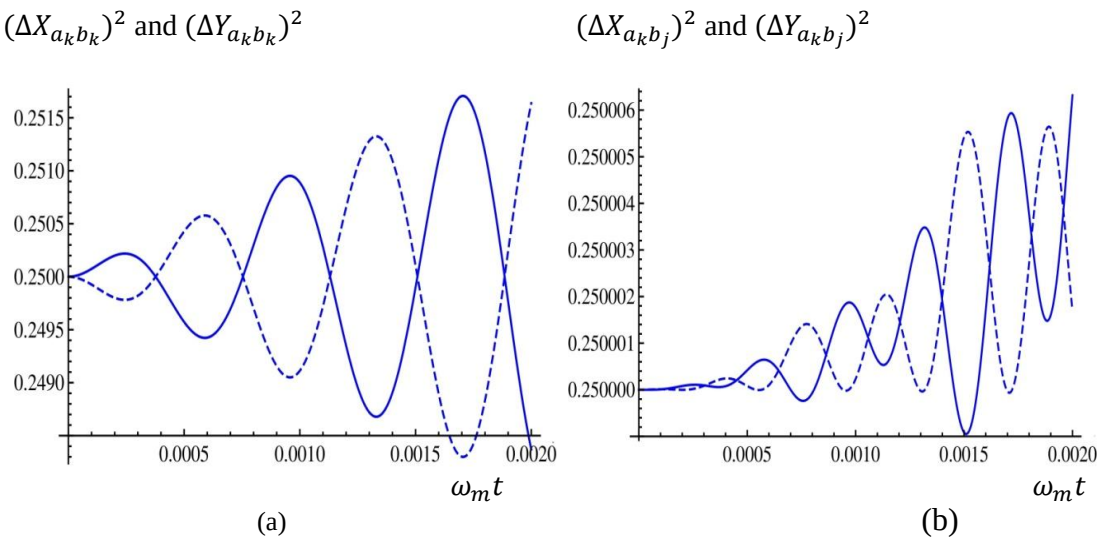

Figure 4.5: Qudrature variation (a) $(\Delta X_{a_k b_k})^2$ (solid line) and $(\Delta Y_{a_k b_k})^2$ (dashed line) for compound mode $a_k b_k$ with $\omega_m t$ for $|\alpha_k| = 6$, $|\beta_k| = 2$ (b) $(\Delta X_{a_k b_j})^2$ (solid line) and $(\Delta Y_{a_k b_j})^2$ (dashed line) for compound mode $a_k b_j$ with $\omega_m t$ for $|\alpha_k| = 6$, $|\beta_j| = 2$. The other parameters are $g/\omega_m = 0.3$, $g/\xi = 4$, $g = 2\pi \times 0.4$ MHz.

Figure 4.5 (b) displays the quadrature variation of $a_k b_j$ inter-mode as a function of normalized time. The dependence of photon tunneling strength and coupling strength on the variance of the quadrature is described as follows: compound mode squeezing is possible for higher value of photon tunneling strength (few MHz). Again, consider photon tunneling strength (graphical condition) as constant, if we lower the value of coupling strength from parametric condition then the degree of squeezing decreases. For coupling strength of the order of KHz, the degree of squeezing is so lowered that its detection is very difficult. The higher value of coupling strength is order of few MHz, compound mode squeezing is ruled out. The fluctuation part of equation (4.13) is very small, so squeezing for $a_k a_j$ inter-mode is not detectable. From equation (4.14), it is clear that, there is no signature of compound mode squeezing for $b_k b_j$ inter-mode.

4.5 Particle statistics

In this section, we have analyzed the particle statistics for cavity field mode and mechanical mode for present system. These particle statistics are studied for single and compound mode in both lower as well as higher order.

4.5.1 Lower order antibunching

Using equation (2.19) and solutions of equation (4.3), we obtain the following analytical expressions of nonclassical factor for single field mode.

$$A_{a_k} = 2|A_2|^2 \mid \alpha_k \mid^4 + \{A_1^{*2}(A_9 A_1 + A_2 A_3)\alpha_k{}^4 + c.c.\} \quad (4.15)$$

$$A_{b_k} = 2|B_2|^2 \mid \alpha_k \mid^2 \mid \beta_k \mid^2 + (B_2^{*2} B_1^2 \mid \alpha_k \mid^2 \beta_k^2 + c.c.) \quad (4.16)$$

Equation (4.15) and (4.16) correspond to expressions for cavity field and mechanical mode, respectively. For all possible values of the interaction parameters the values of A_{a_k} and A_{b_k} are always positive. So, the photon and phonon statistics are super-Poissonian. Using inequality of equation (2.20) and solutions of equation (4.3) we have derived the following expressions of nonclassical factor for different compound mode $a_k b_k$, $a_k b_j$, $a_k a_j$ and $b_k b_j$.

$$A_{a_k b_k} = 2|A_2|^2 \mid \alpha_k \mid^2 (1 + \mid \beta_k \mid^2) \pm$$

$$\left[\{(A_2^* A_1 \beta_k + A_4^* A_2 \beta_k^* + A_7^* A_1 |\beta_k|^2)|\alpha_k|^2 + A_{10}^* A_1 \alpha_j^* \alpha_k \beta_k\} + c.c.\right] \quad (4.17)$$

$$A_{a_k b_j} = A_{11}^* A_1 \alpha_j^* \alpha_k \beta_j + c.c. \quad (4.18)$$

$$A_{a_k a_j} = A_{b_k b_j} = 0 \quad (4.19)$$

As right side of the expressions of equation (4.17) and (4.18) are not simple, so we have plotted these in figure 4.6 (a) and (b), respectively. The negative values of both $A_{a_k b_k}$

and $A_{a_k b_j}$ give the signature of sub-Poissonian statistics i.e. intra photon-phonon and inter photon-phonon antibunching. The degree of antibunching for $a_k b_k$ intra-mode is more compared to $a_k b_j$ intra-mode.

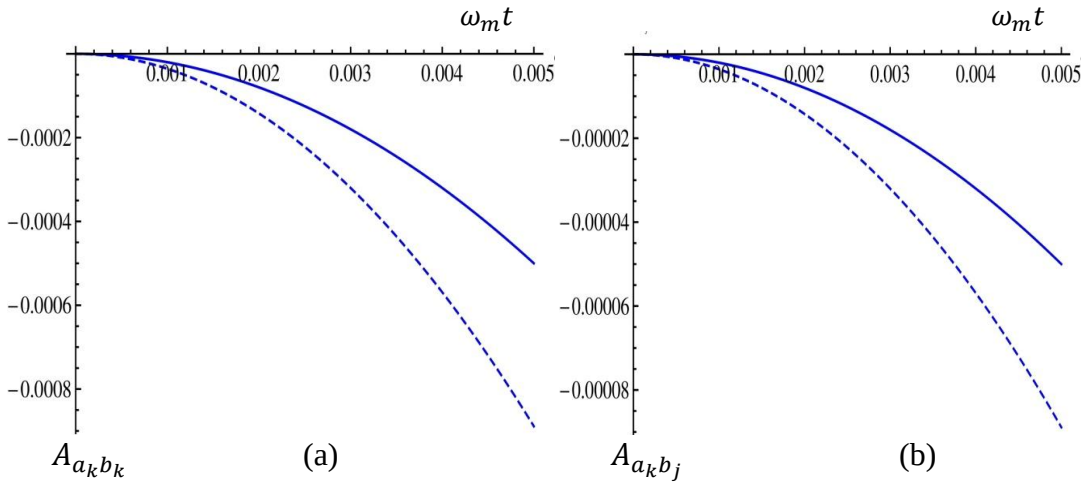

Figure 4.6: Variation of antibunching factors (a) $A_{a_k b_k}$ for compound mode $a_k b_k$ for $|\alpha_k| = 6$, $|\beta_k| = 2$ (solid line) and $|\alpha_k| = 8$, $|\beta_k| = 2$ (dashed line) and (b) $A_{a_k b_j}$ for compound mode $a_k b_j$ for $|\alpha_k| = 6$, $|\beta_j| = 2$ (solid line) and $|\alpha_k| = 8$, $|\beta_j| = 2$ (dashed line) with $\omega_m t$. The other parameters are $g/\omega_m = 0.3$, $g/\xi = 4$, $g = 2\pi \times 0.4$ MHz.

For $a_k b_k$ intra-mode, the degree of nonclassicality does not depend on photon hopping interaction strength, for a constant value of coupling strength. Again, keeping photon tunneling strength constant if we increase the value of coupling strength to several MHz, the intermodal antibunching occurs. For $a_k b_j$ inter-mode the degree of antibunching increases with photon tunneling strength. The degree of nonclassicality also depends upon the weight factor of the input state as shown in figure 4.6. From the expressions (equation 4.17 and 4.18) it can be stated that degree of nonclassicality can be controlled by phase of the input state of the first cavity i.e. replace α_1 by $|\alpha_1| e^{i\varphi}$. The equation (4.19) suggests that there is no signature of intermodal antibunching for $a_k a_j$ and $b_k b_j$ inter-modes.

4.5.2 Higher order antibunching

We examine the possibility of higher order antibunching using Lee criteria (equation 2.22 and 2.24) and solutions of equation (4.3). We obtain the expressions for different single and compound field modes as follows:

$$A_{a_k}(n) = n(n-1)|A_2|^2 \mid \alpha_k \mid^{2n} + \left[nA_1^{*2}\left\{\frac{(n-1)}{2}A_9A_1 + nA_2A_3 \mid \alpha_k \mid^{2n}\right\} \mid \alpha_k \mid^{2n} + c.c.\right] \quad (4.20)$$

$$A_{b_k}(n) = n\left[(n-1)|A_2|^2 \mid \alpha_k \mid^{2n} \mid \beta_k \mid^{2n-2} + \left\{B_2^{*2}B_1^2\left(1 - \frac{n-3}{2} \mid \alpha_k \mid^2\right)|\alpha_k|^{2n}\,|\beta_k|^{n}\,|\beta_k|^{(n-2)} + c.c.\right\}\right] \quad (4.21)$$

Right side of the expressions (equation 4.20 and 4.21) are always positive for a set of system parameters. So, from the analysis it is observed that single mode antibunching is not possible in higher order.

$$\begin{aligned} A_{a_kb_k}(n) = {} & n(n-3)|A_2|^2 \mid \alpha_k \mid^{2n} \mid \beta_k \mid^{2n} \\ & + \left[\frac{n}{2}\{(n-1)(2n+1)|\alpha_k|^2 + n^3\}(B_2^*B_1\beta_k + c.c.)^2\right. \\ & \left. + n^2(B_2^*B_1\beta_k + c.c.)|\beta_k|^2 - \frac{n^3}{2}(B_2^{*2}B_1^2\beta_k^2 + c.c.)\right]|\alpha_k|^{2n}|\beta_k|^{2n-4} \\ & + 2n^2|B_2|^2\left[n^2\{A_{10}^*A_1 + (n-1)A_4^*A_2^*A_1^2\}\alpha_j^*\alpha_k\beta_k + n^3A_2^*A_4\alpha_k^*\alpha_j\beta_k\right. \\ & \left. + c.c.\right]|\alpha_k|^{2n+2}|\beta_k|^{2n-2} \end{aligned} \quad (4.22)$$

$$\begin{aligned} A_{a_kb_j}(n) = {} & n(n-3)|A_2|^2 \mid \alpha_k \mid^{2n} \mid \beta_j \mid^{2n} \\ & + \frac{n(n-1)}{2}(B_2^*B_1\beta_k + c.c.)^2\left|\alpha_j\right|^2|\alpha_k|^{2n}\left|\beta_j\right|^{2n-4} \\ & + n^2\left(A_{11}^*A_1\alpha_j^*\alpha_k\beta_J + c.c.\right)|\alpha_k|^{2n-2}\left|\beta_j\right|^{2n-2} \end{aligned} \quad (4.23)$$

$$A_{a_k a_j}(n) = 2n(n-3)|A_2|^2 \mid \alpha_k \mid^{2n} \mid \alpha_j \mid^{2n} + \frac{n(n-1)}{2}\Big[n(n-1)\left(A_1^{*2}A_4^2\left|\alpha_j\right|^2|\alpha_k|^2 + c.c.\right) + 2n\left(A_1^{*2}A_4^2|\alpha_k|^2 + A_1^{*2}A_4^2\left|\alpha_j\right|^2\right)\alpha_j^{*2}\alpha_k^2\Big]|\alpha_k|^{2n-4}\left|\alpha_j\right|^{2n-4} \quad (4.24)$$

$$A_{b_k b_j}(n) = \frac{n(n-1)}{2}\Big[(B_2^*B_1\beta_k + c.c.)^2|\alpha_k|^2\left|\beta_j\right|^4 + (B_2^*B_1\beta_j + c.c.)^2\left|\alpha_j\right|^2|\beta_k|^4\Big]|\beta_k|^{2n-4}\left|\beta_j\right|^{2n-4} \quad (4.25)$$

The equations (4.22, 4.23, 4.24 and 4.25) provide the analytical expressions of n-th order antibunching for $a_k b_k$, $a_k b_j$, $a_k a_j$ and $b_k b_j$ inter-modes, respectively.

To analyze these, we have plotted the right side of equations (4.22, 4.23 and 4.24) in figure 4.7, for phase angle of $0, \pi/2$ and π of α_k . Figure (a) and (b) display the temporal evolution of intra-cavity photon-phonon $(a_k b_k)$ compound mode. The nonclassical correlation factor shows the negative values for all phase angles. The statistics is sub-Poissonian in nature. Figure (c) depicts the variation of inter-cavity photon-phonon $(a_k b_j)$ compound mode. Degree of antibunching is maximum for phase angle 0 and decreases as phase angle increases. For both the cases the degree of nonclassical correlation factor increases with order number. The variation of $A_{a_k a_j}$ with dimensionless time gt for phase angle 0 and $\pi/2$. It is observed that $A_{a_k a_j}$ is negative and this indicates the signature of photon-photon antibunching (Figure 4.7d). The degree of antibunching is remain same for all phase angle of the input. Interestingly, lower order study shows that there is no signature of intermodal antibunching for $a_k a_j$ compound mode but higher order study shows possibility of sub-Poissonian statistics. From equation (4.25), it is examined that the value of $A_{b_k b_j}$ for all higher order is positive. So, the phonon-phonon intermodal antibunching is not possible for the present system.

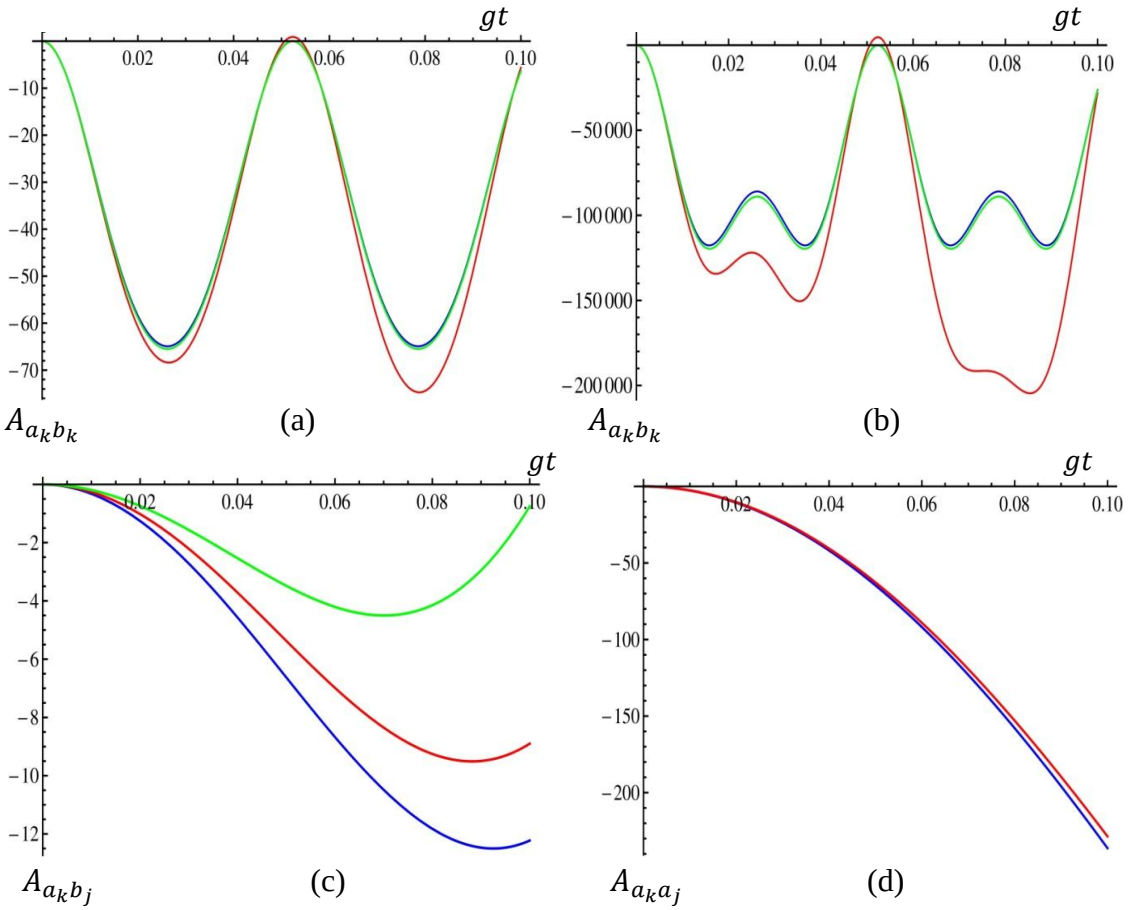

Figure 4.7: Variation of antibunching factors for different compound mode with rescaled time gt (a) $A_{a_k b_k}$ for compound mode $a_k b_k$ for $|\alpha_k| = 3$, $|\beta_k| = 2$, $n = 2$, $g/\omega_m = 0.08$, $g/\xi = 2.5$, $g = 2\pi \times 0.01$ MHz and phase angle 0 (blue line), $\pi/2$ (red line), π (green line) (b) $A_{a_k b_k}$ for compound mode $a_k b_k$ for $|\alpha_k| = 3$, $|\beta_k| = 2$, $n = 4$, $g/\omega_m = 0.08$, $g/\xi = 2.5$, $g = 2\pi \times 0.01$ MHz and phase angle 0 (blue line), $\pi/2$ (red line), π (green line) (c) $A_{a_k b_j}$ for compound mode $a_k b_j$ for $|\alpha_k| = 3$, $|\beta_k| = 2$, $n = 2$, $g/\omega_m = 0.8$, $g/\xi = 4$, $g = 2\pi \times 0.1$ MHz and phase angle 0 (blue line), $\pi/2$ (red line), π (green line) and (d) $A_{a_k a_j}$ for compound mode $a_k a_j$ for $|\alpha_k| = 3$, $|\beta_k| = 2$, $n = 2$, $g/\omega_m = 0.8$, $g/\xi = 4$, $g = 2\pi \times 0.1$ MHz and phase angle 0 (blue line), $\pi/2$ (red line).

4.6 Intermodal Entanglement

In order to investigate intermodal entanglement both in lower as well as higher order, we use Duan et al criteria (equation 2.26), Hillery-Zubairy criteria (equation 2.27, 2.28,

2.29 and 2.30). Intermodal entanglement between four cavity field modes and mechanical modes are studied via two mode entanglement, three and four mode entanglement.

4.6.1 Lower order two mode entanglement

We have derived following expressions for entanglement parameter by using Duan et al criteria (equation 2.26) and solutions of the Hamiltonian (equation 4.3).

$$e_{a_k b_k} = |A_3|^2 + |A_4|^2 + 2|A_2|^2(|\alpha_k|^2 + |\beta_k|^2) + 2|B_2|^2 |\alpha_k|^2 + \{A_1^*(A_6 + A_{14} + A_7 |\beta_k|^2 + 2A_9 |\alpha_k|^2) + B_2^{*2} |\alpha_k|^2 + c.c.\} \quad (4.26)$$

$$e_{a_k b_j} = |A_3|^2 + |A_4|^2 + 2|A_2|^2(|\alpha_k|^2 + |\beta_k|^2) + 2|B_2|^2 |\alpha_j|^2 + \left\{A_1^*(A_6 + A_{14} + A_7 |\beta_k|^2 + 2A_9 |\alpha_k|^2) + B_2^{*2} |\alpha_j|^2 + c.c.\right\} \quad (4.27)$$

$$e_{a_k a_j} = 2|A_3|^2 + 2|A_4|^2 + 2|A_2|^2\left(|\alpha_k|^2 + |\beta_k|^2 + |\alpha_j|^2 + |\beta_j|^2\right) + \left[A_1^*\left\{2A_6 + 2A_{14} + A_7\left(|\beta_k|^2 + |\beta_j|^2\right) + 2A_9\left(|\alpha_k|^2 + |\alpha_j|^2\right)\right\} + c.c.\right] \quad (4.28)$$

$$e_{b_k b_j} = 2|B_2|^2\left(|\alpha_k|^2 + |\alpha_j|^2\right) + \left\{B_2^{*2}\left(|\alpha_k|^2 + |\alpha_j|^2\right) + c.c.\right\} \quad (4.29)$$

Figure 4.8 (a) and (b) depict the temporal variation of entanglement factor $e_{a_k b_k}$ and $e_{a_k b_j}$ (equation 4.26 and 4.27) for intra-cavity and inter-cavity photon-phonon compound mode. The factors are oscillating periodically in between nonclassical and classical regime. The degree of entanglement is enriched with weight factor of the input state. The amplitude of the fluctuation increases due to termination of the calculation up-to second order of the interaction parameter. From equation (4.28) and (4.29), it is observed that the right side is always positive. So, non-separability between two cavity field modes $(a_k a_j)$ and two mechanical modes $(b_k b_j)$ are not possible according to Duan et al criteria.

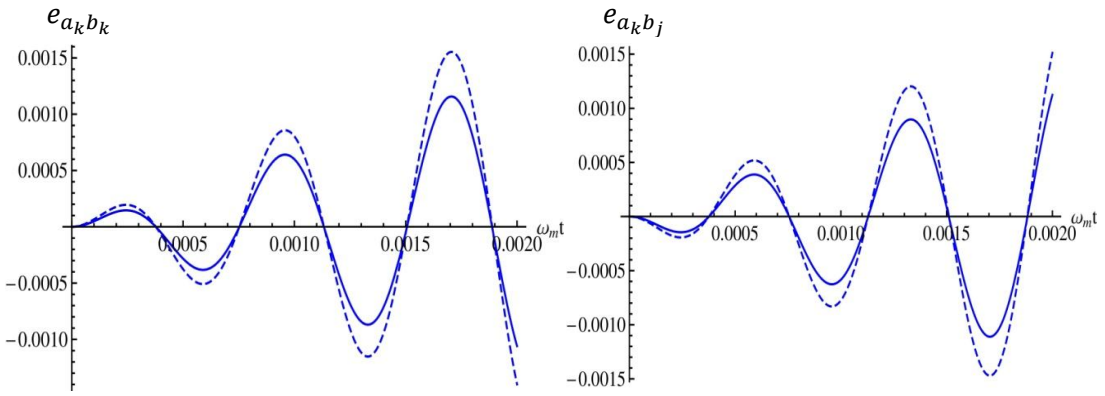

(a) (b)

Figure 4.8: Variation of entanglement parameters (a) $e_{a_k b_k}$ for compound mode $a_k b_k$ for $|\alpha_k| = 6$, $|\beta_k| = 2$ (solid line) and $|\alpha_k| = 8$, $|\beta_k| = 2$ (dashed line) and (b) $e_{a_k b_j}$ for compound mode $a_k b_j$ for $|\alpha_k| = 6$, $|\beta_j| = 2$ (solid line) and $|\alpha_k| = 8$, $|\beta_j| = 2$ (dashed line) with $\omega_m t$. The other parameters are $g/\omega_m = 0.3$, $g/\xi = 4$, $g = 2\pi \times 0.4$ MHz.

Using solutions of equation (4.3) and Hillery-Zubairy entanglement criteria (equation 2.27 and 2.28), we obtain

$$E_{a_k b_k} = \{|A_2|^2 \mid \beta_k \mid^2 + |B_2|^2 \mid \alpha_k \mid^2 + |A_3|^2(1 + \mid \alpha_k \mid^2)\} \mid \alpha_k \mid^2 + \{(A_2^* A_1 \mid \alpha_k \mid^2 + A_{10}^* A_1 \alpha_j^* \alpha_k + A_2^* A_4 \alpha_k^* \alpha_j)\beta_k + c.c.\} \quad (4.30)$$

$$E_{a_k b_j} = \{(|A_2|^2 \mid \beta_j \mid^2 + |B_2|^2 \mid \alpha_j \mid^2) \mid \alpha_k \mid^2 + (A_{11}^* A_1 \beta_j - A_{12}^* A_1 \beta_j^*)\alpha_j^* \alpha_k\} + \{B_1^* B_2 (A_1^* A_4 \alpha_k^* \alpha_j - A_4^* A_1 \alpha_j^* \alpha_k) + B_1^* B_4 (\alpha_k^* \alpha_j + \alpha_j^* \alpha_k)\}\beta_j^* \quad (4.31)$$

$$E_{a_k a_j} = 2|A_2|^2 \mid \alpha_k \mid^2 \mid \alpha_j \mid^2 \quad (4.32)$$

$$E_{b_k b_j} = |B_2|^2 (\mid \alpha_k \mid^2 \mid \beta_j \mid^2 + \mid \alpha_j \mid^2 \mid \beta_k \mid^2) \quad (4.33)$$

$$E'_{a_k b_k} = \{|A_2|^2 \mid \beta_k \mid^2 - |B_2|^2(1 + \mid \alpha_k \mid^2)\} \mid \alpha_k \mid^2 - \{(B_1^* B_2 \mid \alpha_k \mid^2 + B_1^* B_3 \alpha_k^* \alpha_j + A_4^* A_2 B_1^* B_2 \alpha_j^* \alpha_k)\beta_k^* + c.c.\} \quad (4.34)$$

$$E'_{a_k b_j} = (|A_2|^2 \mid \beta_j \mid^2 + |B_2|^2 \mid \alpha_j \mid^2) \mid \alpha_k \mid^2$$

$$+\{(A_4B_2 + A_1B_4)A_1^*B_1^*\alpha_k^*\alpha_j\beta_j^* + c.c.\} \quad (4.35)$$

$$E'_{a_ka_j} = E_{a_ka_j} \quad ; \quad E'_{b_kb_j} = E_{b_kb_j} \quad (4.36)$$

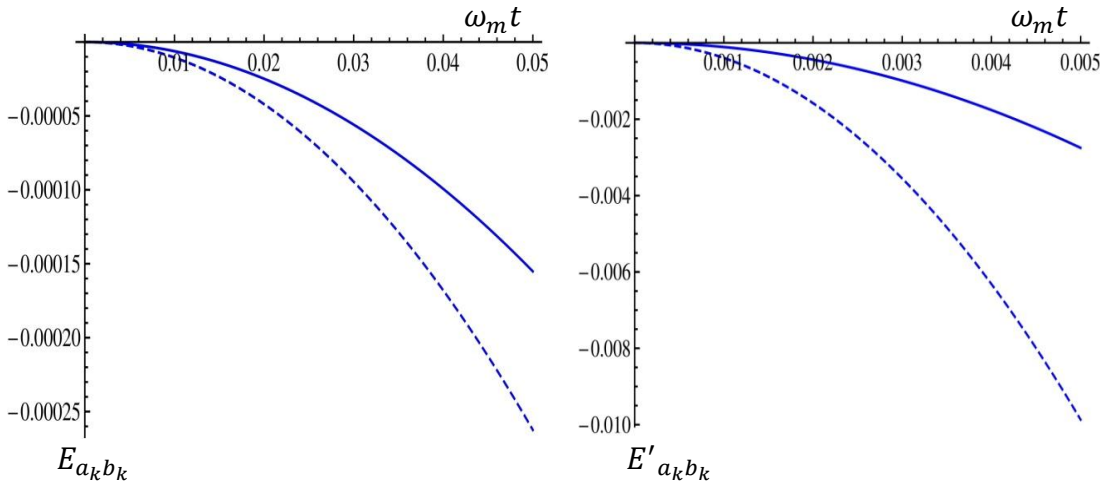

(a) (b)

Figure 4.9: Variation of (a) $E_{a_kb_k}$ with $\omega_m t$ for $g/\omega_m = 0.001, g/\xi = 0.012$, $g = 2\pi \times 1.2$ MHz, $|\alpha_k| = 6$, $|\beta_k| = 2$ (solid line) and $|\alpha_k| = 8$, $|\beta_k| = 2$ (dashed line) and (b) $E'_{a_kb_k}$ with $\omega_m t$ for $g/\omega_m = 0.3, g/\xi = 4$, $g = 2\pi \times 0.4$ MHz, $|\alpha_k| = 6$, $|\beta_k| = 2$ (solid line) and $|\alpha_k| = 8$, $|\beta_k| = 2$ (dashed line).

The graphical representation of equation (4.30) and (4.34), are shown in figure 4.9 (a) and (b), respectively. Both the Hillery-Zubairy criteria have shown that non-separable state exists for a_kb_k intra-mode as the values of $E_{a_kb_k}$ and $E'_{a_kb_k}$ are negative. Keeping photon tunneling strength constant (parametric condition), if we increase the coupling strength, the degree of entanglement increases. The upper-limit of coupling strength is few hundred KHz, beyond that entangled state is ruled out. The right side of equations (4.31, 4.32, 4.33, 4.35 and 4.36) is positive for any values of system parameters. So, there is no signature of intermodal entanglement for inter-cavity photon-phonon

mode($a_k b_j$), inter-cavity photon-photon mode($a_k a_j$) and inter-cavity phonon-phonon mode($b_k b_j$) .

4.6.2 Higher-order two mode entanglement

Higher order two mode entanglement is investigated by using Hilery-Zubairy criteria (equation 2.30 and 2.31). Using these criteria and solutions of equation (4.3), we obtain the expressions for nonclassical correlation factors as

$$\begin{aligned} E_{a_k b_k}^{m,n} = \big[&\{m^2|A_2|^2|\beta_k|^2 + n^2|B_2|^2|\alpha_k|^2 + mn|A_3|^2(1+2|\alpha_k|^2)\}|\alpha_k|^2 \\ &+ mn\{(A_2^* A_1|\alpha_k|^2 + A_{10}^* A_1 \alpha_j^* \alpha_k + A_2^* A_4 \alpha_k^* \alpha_j)\beta_k + c.c.\} \\ &+ mn(m-1)\{(A_2^* A_4 \beta_k + c.c.)\alpha_k^* \alpha_j\}\big]|\alpha_k|^{2m-2}|\beta_k|^{2n-2} \\ &+ mn(n-1)\{(A_5^* A_1 {\beta_k}^2 + c.c.)(2|\alpha_k|^2 + m) + |A_3|^2|\beta_k|^2(1 \\ &+ 2|\alpha_k|^2)\}|\alpha_k|^{2m}|\beta_k|^{2n-4} \end{aligned} \tag{4.37}$$

$$\begin{aligned} E_{a_k b_j}^{m,n} = \big[&\left(m^2|A_2|^2|\beta_j|^2 + n^2|B_2|^2|\alpha_j|^2\right)|\alpha_k|^2 \\ &+ mn\{A_1(A_{11}^* \beta_j - A_{12}^* {\beta_j}^*)\alpha_j^* \alpha_k + B_1^* B_2(A_1^* A_4 \alpha_k^* \alpha_j - A_4^* A_1 \alpha_j^* \alpha_k){\beta_j}^* \\ &+ B_1^* B_4(\alpha_k^* \alpha_j + c.c.){\beta_j}^*\}\big]|\alpha_k|^{2m-2}|\beta_j|^{2n-2} \end{aligned} \tag{4.38}$$

$$E_{a_k b_j}^{m,n} = (m^2+n^2)|A_2|^2|\alpha_k|^{2m}|\alpha_j|^{2n} \tag{4.39}$$

$$E_{b_k b_j}^{m,n} = |B_2|^2\left[m^2|\alpha_k|^2|\beta_j|^2 + n^2|\alpha_j|^2|\beta_k|^2\right]|\beta_k|^{2m-2}|\beta_j|^{2n-2} \tag{4.40}$$

$$\begin{aligned} E'^{m,n}_{a_k b_k} = \big[&m^2|A_2|^2|\beta_k|^2 - n^2|B_2|^2\{(2m-1)|\alpha_k|^2 + m^2\}|\alpha_k|^2 \\ &- mn\{(B_1^* B_2|\alpha_k|^2 + B_1^* B_3 \alpha_k^* \alpha_j + B_1^* B_2 A_4^* A_2 \alpha_j^* \alpha_k){\beta_k}^* \\ &+ (m-1)A_1^* A_4 B_1^* B_2 \alpha_k^* \alpha_j {\beta_k}^* + c.c.\}\big]|\alpha_k|^{2m-2}|\beta_j|^{2n-2} \end{aligned} \tag{4.41}$$

$$\begin{aligned} E'^{m,n}_{a_k b_j} = \big[&\left(m^2|A_2|^2|\beta_j|^2 + n^2|B_2|^2|\alpha_j|^2\right)|\alpha_k|^2 \\ &+ mn\{(A_4 B_2 + A_1 B_4)A_1^* B_1^* \alpha_k^* \alpha_j {\beta_j}^* + c.c.\}\big]|\alpha_k|^{2m-2}|\beta_j|^{2n-2} \end{aligned} \tag{4.42}$$

$$E'^{m,n}_{a_k a_j} = E^{m,n}_{a_k a_j} \quad ; \quad E'^{m,n}_{b_k b_j} = E^{m,n}_{b_k b_j} \tag{4.43}$$

For $m = n$ the above equations are taken the form

$$\begin{aligned} E^{n,n}_{a_k b_k} = \big[& n^2 E_{a_k b_k} + n^2(n-1)\{(A_2^* A_4 \beta_k + c.c.)\alpha_k^* \alpha_j\}\big]|\alpha_k|^{2n-2}|\beta_k|^{2n-2} \\ & + n^2(n-1)\{(A_5^* A_1 {\beta_k}^2 + c.c.)(2|\alpha_k|^2 + n) + |A_3|^2|\beta_k|^2(1 \\ & + 2|\alpha_k|^2)\}|\alpha_k|^{2n}|\beta_k|^{2n-4} \end{aligned} \tag{4.44}$$

$$E^{n,n}_{a_k b_j} = n^2 E_{a_k b_j}|\alpha_k|^{2n-2}\left|\beta_j\right|^{2n-2} \tag{4.45}$$

$$E^{n,n}_{a_k a_j} = n^2 E_{a_k a_j}|\alpha_k|^{2n-2}\left|\alpha_j\right|^{2n-2} \tag{4.46}$$

$$E^{n,n}_{b_k b_j} = 2n^2 E_{b_k b_j}|\beta_k|^{2n-2}\left|\beta_j\right|^{2n-2} \tag{4.47}$$

$$\begin{aligned} E'^{n,n}_{a_k b_k} = \big[& n^2 E_{a_k b_k} \\ & - (n-1)\{2n^2|B_2|^2|\alpha_k|^2 - A_1^* A_4 B_1^* B_2 \alpha_k^* \alpha_j {\beta_k}^* \\ & + c.c.\}\big]\,|\alpha_k|^{2n-2}\left|\beta_j\right|^{2n-2} \end{aligned} \tag{4.48}$$

$$E'^{n,n}_{a_k b_j} = n^2 E'_{a_k b_j}|\alpha_k|^{2n-2}\left|\beta_j\right|^{2n-2} \tag{4.49}$$

$$E'^{n,n}_{a_k a_j} = E^{n,n}_{a_k a_j} \quad ; \quad E'^{n,n}_{b_k b_j} = E^{n,n}_{b_k b_j} \tag{4.50}$$

To illustrate the possibility of higher-order entanglement in present system we analyze equation (4.44) to (4.50). We plot the equations (4.44) and (4.48) in figure 4.10 (a) and (b), respectively. The negativity of $E^{m,n}_{a_k b_k}$ and $E'^{m,n}_{a_k b_k}$ gives the signature of higher order entanglement in $a_k b_k$ intra-cavity photon-phonon mode. The degree of entanglement is enhanced as compared to lower order (Figure 4.9). The right side of equations (4.45,

4.46, 4.47, 4.49 and 4.50) is positive for possible values of interaction parameters. So, higher-order entanglement is not observed for $a_k b_j$, $a_k a_j$ and $b_k b_j$ inter-modes.

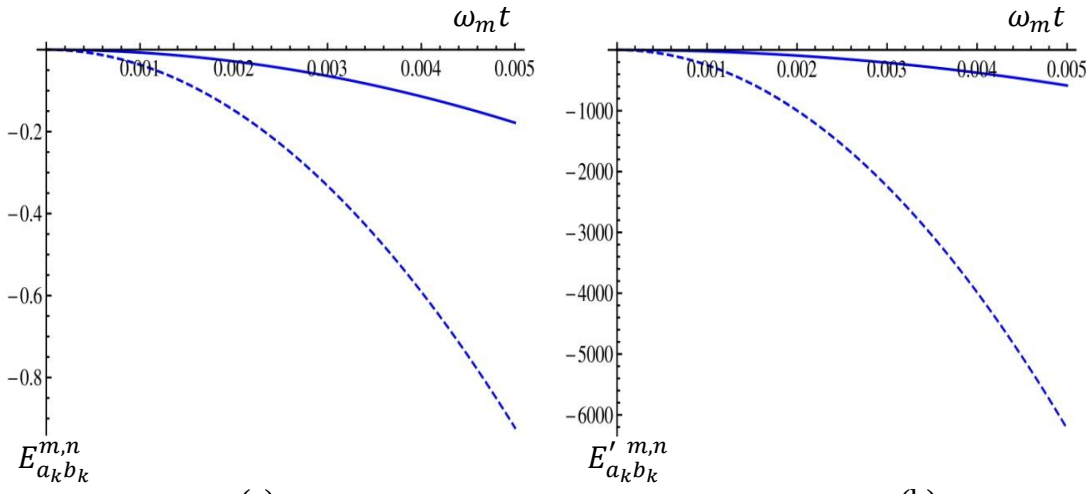

(a) (b)

Figure 4.10: Variation of (a) $E^{m,n}_{a_k b_k}$ with $\omega_m t$ for $g/\omega_m = 0.001, g/\xi = 0.012$, $g = 2\pi \times 1.2$ MHz, $m = n = 3$, $|\alpha_k| = 6$, $|\beta_k| = 2$ (solid line) and $|\alpha_k| = 8$, $|\beta_k| = 2$ (dashed line) and (b) $E'^{m,n}_{a_k b_k}$ with $\omega_m t$ for $g/\omega_m = 0.3, g/\xi = 4$, $g = 2\pi \times 0.4$ MHz, $m = n = 3$, $|\alpha_k| = 6$, $|\beta_k| = 2$ (solid line) and $|\alpha_k| = 8$, $|\beta_k| = 2$ (dashed line).

4.6.3 Three mode entanglement

We examine the intermodal entanglement via three field mode entanglement. This is a type of higher order entanglement. Using moment based inequality of Li et al criterion 1 (equation 2.34), we obtain the analytical expressions of ζ_1, ζ_2, ζ_3 and ζ_4, which correspond to three field inter-modes $a_k b_k b_j$, $a_k b_j b_k$, $a_k a_j b_j$ and $a_j a_k b_j$, respectively.

$$\zeta_1 = |\alpha_k|^2 |\beta_j|^2 \left(|\alpha_k|^2 + |\alpha_j|^2\right) |B_2|^2 + |\alpha_k|^2 |\beta_k|^2 |\beta_j|^2 |A_3|^2 + \left(\alpha_j^* \alpha_k \beta_k |\beta_j|^2 A_{11}^* A_1 + c.c.\right) \quad (4.51)$$

$$\begin{aligned}\zeta_2 = {} & |\alpha_k|^2 |\beta_j|^2 (1 + |\beta_k|^2) |A_3|^2 + |\alpha_k|^2 \left(|\alpha_k|^2 |\beta_j|^2 + |\alpha_j|^2 |\beta_k|^2\right) |B_2|^2 \\ & + \left(|\alpha_k|^2 |\beta_j|^2 \beta_k A_2^* A_1 + |\alpha_k|^2 |\alpha_j|^2 \beta_j \beta_k A_2^* A_1 B_2^* B_1 \right. \\ & + \alpha_k^* \alpha_j \beta_k |\beta_j|^2 A_2^* A_4 + |\alpha_k|^2 |\alpha_j|^2 \beta_j^* \beta_k A_2^* A_1 B_1^* B_2 \\ & \left. + \alpha_j^* \alpha_k \beta_k |\beta_j|^2 A_{10}^* A_1 + |\alpha_k{}^2|^2 |\beta_j|^2 A_2^* A_1 B_1^* B_2 + c.c.\right) \end{aligned} \quad (4.52)$$

$$\zeta_3 = 2 \mid \alpha_k \mid^2 \mid \beta_j \mid^2 \mid \alpha_j \mid^2 \mid A_2 \mid^2 + \mid \alpha_k \mid^2 \mid \alpha_j{}^2 \mid^2 \mid B_2 \mid^2 + \mid \alpha_j \mid^2 \alpha_j^* \alpha_k \left(\beta_j A_{10}^* A_1 + c.c.\right) - \mid \alpha_k \mid^2 \alpha_k^* \alpha_j \left(\beta_j A_1^* A_{12} + c.c.\right) + \left(\mid \alpha_k \mid^2 \beta_k \mid \alpha_j \mid^2 A_2^* A_1 + \alpha_j^* \alpha_k \beta_j \mid \alpha_k \mid^2 A_2^* A_4 + \mid \alpha_k \mid^2 \mid \alpha_j{}^2 \mid^2 A_2^* A_1 B_1^* B_2 + c.c.\right) \quad (4.53)$$

$$\zeta_4 = 2 \mid \alpha_j \mid^2 \mid \beta_k \mid^2 \mid \alpha_j \mid^2 \mid A_2 \mid^2 + \mid \alpha_j \mid^2 \mid \alpha_k{}^2 \mid^2 \mid B_2 \mid^2 + \left(\mid \alpha_k \mid^2 \beta_k \mid \alpha_j \mid^2 A_2^* A_1 + \mid \alpha_j \mid^2 \mid \alpha_k{}^2 \mid^2 A_2^* A_1 B_1^* B_2 + \alpha_k^* \alpha_j \beta_j \mid \alpha_k \mid^2 A_2^* A_4 + c.c.\right) + \mid \alpha_j \mid^2 \alpha_j^* \alpha_k (\beta_k A_{10}^* A_1 + c.c.) + \mid \alpha_k \mid^2 \beta_k \left(\alpha_k^* \alpha_j A_2^* A_1 A_4^* A_1 + c.c.\right) - \mid \alpha_k \mid^2 \alpha_k^* \alpha_j (\beta_k A_1^* A_{12} + c.c.) \quad (4.54)$$

The right sides of the above expressions are depicted in figure 4.11(a-d). The negative regions of the plots indicate the presence of three mode entangled state. For all cases the entanglement factors vary in a periodic manner, with different degree. The variations of the degree of different entanglement factor with interaction parameters are illustrated as follows: In case of $a_k b_k b_j$ inter-mode, keeping coupling strength constant if we change the photon tunneling strength, it is observed that the lower limit of photon tunneling strength is 16 KHz, entangled state exists. If we increase photon tunneling strength up to few hundred KHz the degree of entanglement is small but considerably increases when photon tunneling strength is order of MHz. In absence of photon tunneling strength the entangled state is ruled out. This is due to fact that, when photon tunneling strength is zero there is no interaction between the cavities. The photon tunneling strength plays the key role to entangle the mechanical modes. Mathematically, the time dependent term $A_{11}^* A_1$ in the equation (4.51), is zero in absence of photon hopping. In presence of photon hopping this term plays important role for negative value of ζ_1 . Again, taking photon hopping term constant, if we increase the value of the coupling strength, it is observed that entangled state is possible up-to few hundred KHz, beyond

that ζ_1 is positive and entangled state is ruled out. For smaller values of coupling strength the degree of entanglement decreases, beyond 1 KHz the degree of entanglement is so smaller, it is difficult to detect. The phase variation of the cavity field modes (replacing α_k and α_j by $|\alpha_k|e^{i\varphi}$ and $|\alpha_j|e^{i\theta}$, respectively) are shown where non-separable state exists for phase angle (i) $\varphi = \pi/4\,, \pi/2\,, 3\pi/4$ and $\theta = 0$ (ii) $\theta = 5\pi/4\,, 3\pi/2$ and $\varphi = 0$. In case of $a_k b_j b_k$ inter-mode, keeping coupling strength constant if we increase photon tunneling strength, the negative value is lowered i.e. degree of it is lowered. If we further increase tunneling strength up to order of MHz, entangled state disappears. Again, for constant value of photon tunneling strength (graphical condition), if we increase coupling strength up-to few hundred KHz, the non-separability is ruled out. Variation of the phase of the input state show that the entangled state exists for the phase angle (i) $\varphi = \pi/4\,, \pi/2\,, 3\pi/4\,, \pi, 5\pi/4\,, 3\pi/2$ and $\theta = 0$ (ii) $\theta = \pi/4\,, \pi/2\,, 3\pi/4\,, \pi, 5\pi/4,\quad 3\pi/2$ and $\varphi = 0$. For $a_k a_j b_j$ inter-mode, taking tunneling strength constant, if we increase coupling strength up-to few hundred KHz, the non-separable state exists, beyond that limit entangled state disappears. Again, considering coupling strength same value, if we lower the tunneling parameter up-to few hundred Hz, the negativity of ζ_3 is remain unaltered. If we increase tunnelling strength up-to few hundred MHz, the entangled state is signed out. Lastly, variation of the entanglement parameter ζ_4 for $a_j a_k b_j$ inter-mode is very similar to $a_k a_j b_j$ inter-mode. But the degree of non-separability for $a_j a_k b_j$ inter-mode is slightly higher as compared to $a_k a_j b_j$ inter-mode.

From the variation of three mode entanglement factors, it is also observed that degree of entanglement is much larger than that of lower order for two mode entanglement. Interestingly, it can also be concluded that non-separability of two mechanical modes

are not observed via two mode inequality but in presence of any cavity field the two mechanical modes are entangled. This study confirms the generation of nonclassicality at macroscopic level.

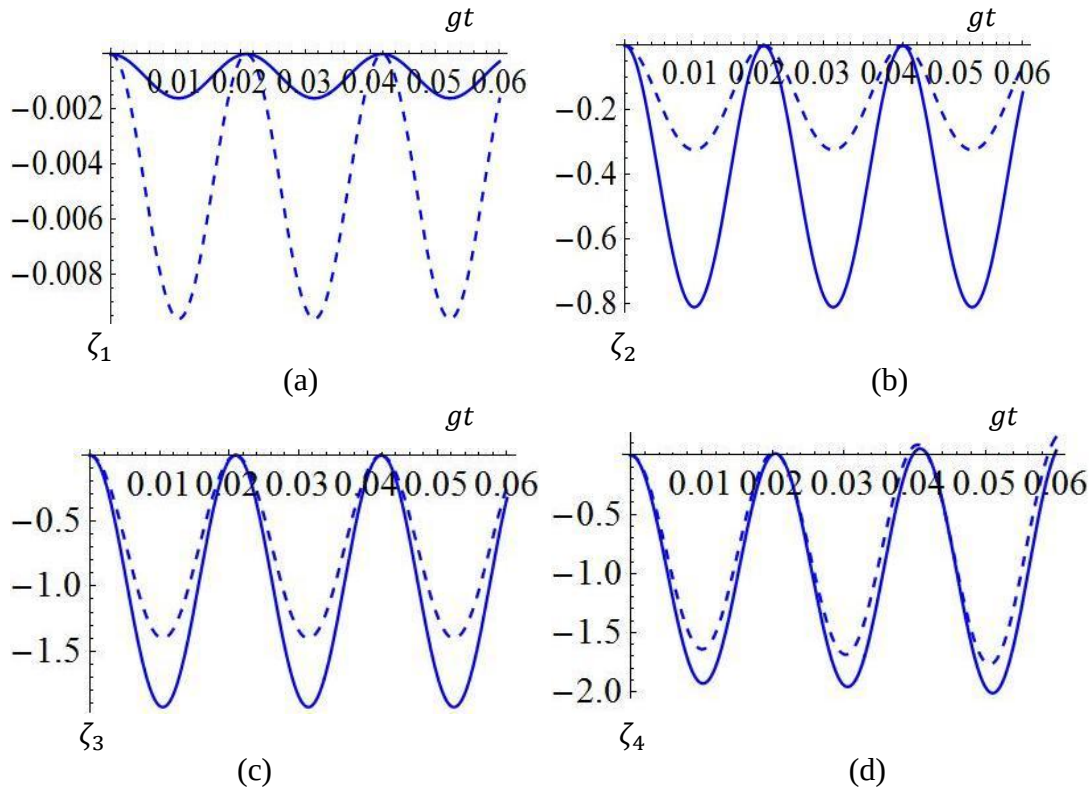

Figure 4.11: Plot of intermodal entanglement factors with normalized time gt for phase angle $\theta_1 = 0$ and $\theta_2 = 0$ (a) ζ_1 for $a_k b_k b_j$ mode (b) ζ_2 for $a_k b_j b_k$ mode (c) ζ_3 for $a_k a_j b_j$ mode (d) ζ_4 for $a_j a_k b_j$ mode. Other parameters are $g/\omega_m = 0.0033$, $g/\xi = 0.12$ and $|\alpha_k| = 3$, $|\alpha_j| = 3$, $|\beta_k| = 2$, $|\beta_j| = 2$ (solid line) ; $|\alpha_k| = 4$, $|\alpha_j| = 3$, $|\beta_k| = 2$, $|\beta_j| = 1$ (dashed line).

Using moment based inequality Li *et al* criterion 2 (equation 2.35) and solutions of equation 4.3, we have derived the analytical expressions of ε_1, ε_2, ε_3 and ε_4 for different three field modes $a_k b_k b_j$, $a_k b_j b_k$, $a_k a_j b_j$ and $a_j a_k b_j$, respectively.

$$\begin{aligned}\varepsilon_1 = &|\alpha_k|^2|\beta_k|^2\left(|\beta_j|^2|A_3|^2+|\alpha_j|^2|B_2|^2\right)+|\alpha_k|^2|\beta_k|^2(1+|\alpha_k|^2)|B_2|^2\\ &-\left\{|\alpha_j|^2|\beta_k|^2\beta_k^*B_1^*B_2+|\alpha_k|^2|\alpha_j|^2\left(\beta_j^*\beta_k^*B_2^2B_1^{*2}+\beta_j^*\beta_k B_2^*B_2\right)\right.\\ &+|\beta_k|^2\left(\alpha_k^*\alpha_j\beta_j^*A_1^*A_4B_1^*B_2+\alpha_j^*\alpha_k\beta_j^*A_4^*A_1B_1^*B_2\right)\\ &\left.+\left(\alpha_k^*\alpha_j|\beta_j|^2\beta_k^*+\alpha_k^*\alpha_j^*|\beta_k|^2\beta_j^*\right)B_1^*B_3+c.c.\right\}\end{aligned} \tag{4.55}$$

$$\varepsilon_2 = |\alpha_k|^2|\beta_j|^2\left(|\beta_k|^2|A_2|^2+|\alpha_j|^2|B_2|^2\right)+|\alpha_k|^2|\beta_j|^2(1+|\alpha_k|^2)|B_2|^2$$
$$-\left\{|\alpha_k|^2|\alpha_j|^2\left(\beta_j^*\beta_k^*B_2^2B_1^{*2}+\beta_j^*\beta_kB_2^*B_2\right)+|\beta_k|^2\alpha_j^*\alpha_k\beta_jA_4^*A_1B_2^*B_1\right.$$
$$+\left(\alpha_j^*\alpha_k|\beta_j|^2\beta_kB_3^*B_1+\alpha_k\alpha_j^*|\beta_k|^2\beta_jB_4^*B_1\right)+|\alpha_k|^2|\beta_j|^2\beta_k^*B_1^*B_2$$
$$\left.+|\beta_j|^2\alpha_k^*\alpha_j\beta_kA_1^*A_4B_1^*B_2+c.c.\right\} \quad (4.56)$$

$$\varepsilon_3 = 2|\alpha_k|^2|\alpha_j|^2|\beta_k|^2|A_3|^2-|\alpha_k|^2|\alpha_j|^2(1+|\alpha_k|^2)|B_2|^2$$
$$-\left\{A_4^*A_1B_2^*B_1\left(|\alpha_k|^2\alpha_k^*\alpha_j\beta_k^*+|\alpha_j|^2\alpha_j^*\alpha_k\beta_k^*\right)\right.$$
$$+|\alpha_k|^2\alpha_j^*\alpha_k\beta_k^*(2A_1^*A_4B_1^*B_2+B_1^*B_4)$$
$$\left.+|\alpha_k|^2|\alpha_j|^2\beta_k^*(B_1^*B_2+B_1^*B_3)+c.c.\right\} \quad (4.57)$$

$$\varepsilon_4 = |\alpha_k|^2|\alpha_j|^2|\beta_k|^2|A_2|^2-|\alpha_j|^2|\alpha_k|^2(1+|\alpha_k|^2)|B_2|^2$$
$$-\left\{|\alpha_k|^2|\alpha_j|^2\beta_k^*(B_1^*B_2+B_1^*B_3)+|\alpha_k|^2\alpha_j^*\alpha_k\beta_k^*(2A_1^*A_4B_1^*B_2\right.$$
$$\left.+B_1^*B_4\right)+A_4^*A_1B_2^*B_1\left(|\alpha_k|^2\alpha_k^*\alpha_j\beta_k^*+|\alpha_j|^2\alpha_j^*\alpha_k\beta_k^*\right)+c.c.\} \quad (4.58)$$

To illustrate the possibility of three mode entanglement using Li et al criteria 2, we have plotted the equations (4.55-4.58) in figures 4.12 (a-d). From the temporal variations (a, b), it is observed that the entanglement factors ε_1, ε_2 are negative for larger value of dimensionless interaction time gt. This confirms the possibility of intermodal entanglement for compound mode $a_kb_kb_j$ and $a_kb_jb_k$. For $a_kb_kb_j$ mode, the entangled state is observed for all possible values of phase angle except $\varphi = 0$ and $\theta = 3\pi/2$. In case of $a_kb_jb_k$ inter-mode the nonclassicality is observed for phase angle (i) $\theta = \pi/4, \pi/2, 3\pi/4$ and for $\varphi = 0$ - degree of entanglement prominent and (ii) $\varphi = \pi, 5\pi/4$ and $\theta = 0$; $\theta = \pi$ and $\varphi = 0$ - degree of entanglement small. From figure (c) it is clear that ε_3 is positive for phase angle $\theta = 0$ and $\varphi = 0$. So, three mode entangled state is not possible for this set of phase angle. If we vary phase of the input state it is observed that ε_3 becomes negative and non-separable state is possible for (i) $\varphi = \pi/4, \pi/2, 3\pi/4, \pi$ and $\theta = 0$ (ii) $\theta = \pi, 4, 3\pi/2$ and $\varphi = 0$. Again, from figure (d) it is clear that very lower possibility of entangled state for $a_ja_kb_j$ mode for phase

angle $\theta = 0$ and $\varphi = 0$. For other possible phases the variation is similar to $a_k a_j b_j$ inter-mode. From these variation it is also stated that degree of entanglement also depend on weight factor of input states.

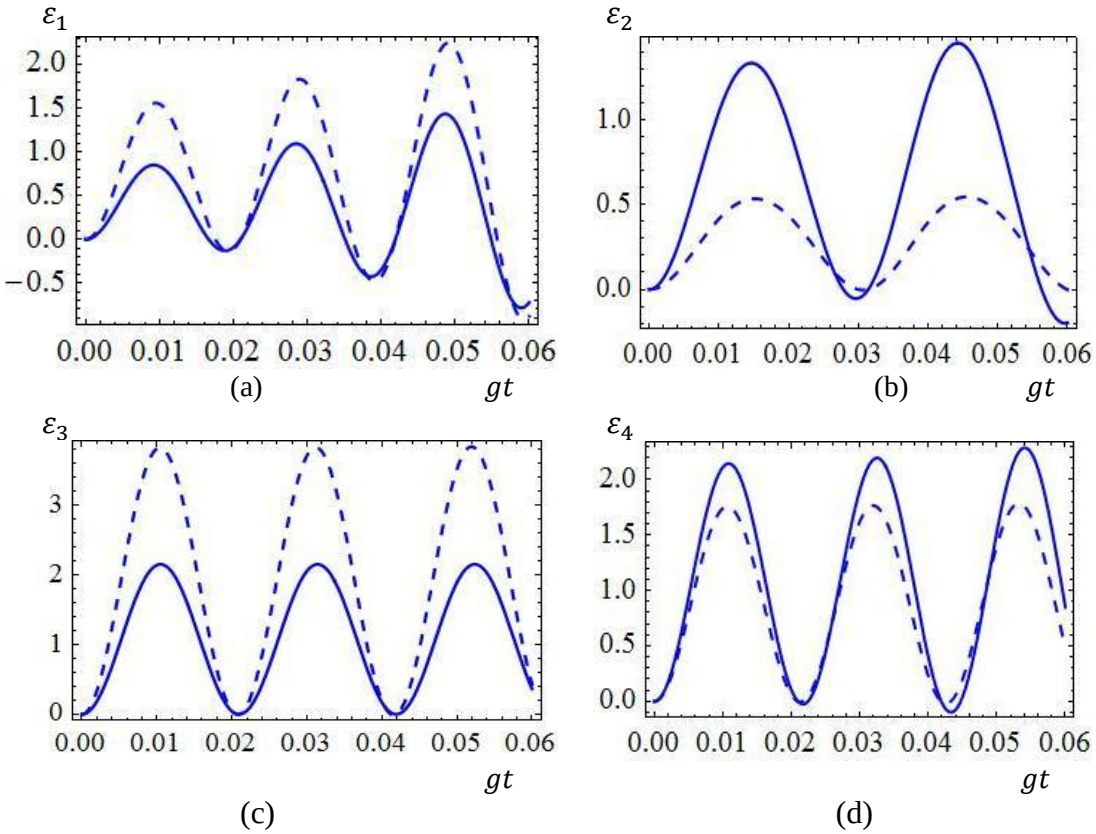

Figure 4.12: Variation of intermodal entanglement factors with normalized time gt for phase angle $\theta_1 = 0$ and $\theta_2 = 0$ (a) ε_1 for $a_k b_k b_j$ mode (b) ε_2 for $a_k b_j b_k$ mode (c) ε_3 for $a_k a_j b_j$ mode (d) ε_4 for $a_j a_k b_j$ mode. Other parameters are $g/\omega_m = 0.0033$, $g/\xi = 0.12$ and $|\alpha_k| = 3$, $|\alpha_j| = 3$, $|\beta_k| = 2$, $|\beta_j| = 2$ (solid line) ; $|\alpha_k| = 4$, $|\alpha_j| = 3$, $|\beta_k| = 2$, $|\beta_j| = 1$ (dashed line).

4.6.4 Four mode entanglement

Here, we have discussed another type of entanglement via four field modes in present system. Using Li et al criteria (2.36) and solutions of equation (4.3), we find the following entanglement factor.

$$E_{a_1b_1a_2b_2} = 2 \mid \alpha_1 \mid^2 \mid \beta_1 \mid^2 \mid \alpha_2 \mid^2 \mid \beta_2 \mid^2 \mid A_2 \mid^2 - (\mid \alpha_1{}^2 \mid^2 \mid \alpha_2 \mid^2 \mid \beta_2 \mid^2 +$$

$$\mid \alpha_2{}^2 \mid^2 \mid \alpha_1 \mid^2 \mid \beta_1 \mid^2 + \mid \alpha_1 \mid^2 \mid \beta_1 \mid^2 \mid \alpha_2 \mid^2 + \mid \alpha_1 \mid^2 \mid \beta_2 \mid^2 \mid \alpha_2 \mid^2) \mid B_2 \mid^2 +$$

$$\mid \alpha_1 \mid^2 \mid \beta_1 \mid^2 \mid \alpha_2 \mid^2 \alpha_1\beta_1\alpha_2 B_1^* B_4 + \mid \alpha_1 \mid^2 \mid \beta_2 \mid^2 \alpha_2^*\alpha_1\beta_1^* A_1^* A_{11} +$$

$$\{\mid \alpha_1{}^2 \mid^2 \mid \alpha_2{}^2 \mid^2 \beta_2^*\beta_1 B_2^* B_2 + (2 \mid \alpha_2 \mid^2 \mid \beta_1 \mid^2 \alpha_1^*\alpha_2\beta_2^* + \mid \alpha_1 \mid^2 \mid \beta_1 \mid^2 \alpha_2^*\alpha_1\beta_2^* +$$

$$\mid \alpha_1 \mid^2 \mid \beta_2 \mid^2 \alpha_2^*\alpha_1\beta_1^*) B_1^* B_2 A_1^* A_4 + \mid \alpha_1 \mid^2 \mid \alpha_2 \mid^2 \beta_2^*\beta_1 B_2^* B_2 +$$

$$(\alpha_1^*\alpha_2 \mid \beta_1 \mid^2 \mid \alpha_2 \mid^2 \beta_1^* + \alpha_1^*\alpha_2 \mid \beta_2 \mid^2 \mid \alpha_2 \mid^2 \beta_2^*) B_1^* B_3 + (\mid \alpha_1 \mid^2 \mid \alpha_2 \mid^2 +$$

$$\mid \alpha_1{}^2 \mid^2 \mid \alpha_2{}^2 \mid^2 + \mid \alpha_2{}^2 \mid^2 \mid \alpha_1 \mid^2) \beta_1^*\beta_2^* B_2^2 B_1^{*2} + (\mid \alpha_1 \mid^2 \mid \beta_2 \mid^2 \mid \alpha_2 \mid^2 \beta_1^* +$$

$$\mid \alpha_1 \mid^2 \mid \beta_1 \mid^2 \mid \alpha_2 \mid^2 \beta_2^*) B_1^* B_2 + \mid \alpha_1 \mid^2 \mid \beta_2 \mid^2 \alpha_2^*\alpha_1\beta_2^* B_2^* B_1 A_1^* A_4 +$$

$$+(\mid \alpha_2 \mid^2 \mid \beta_2 \mid^2 \alpha_2^*\alpha_1\beta_1^* + \mid \alpha_2 \mid^2 \mid \beta_1 \mid^2 \alpha_2^*\alpha_1\beta_2^*) B_1^* B_2 A_4^* A_1 + c.c.\} \qquad (4.59)$$

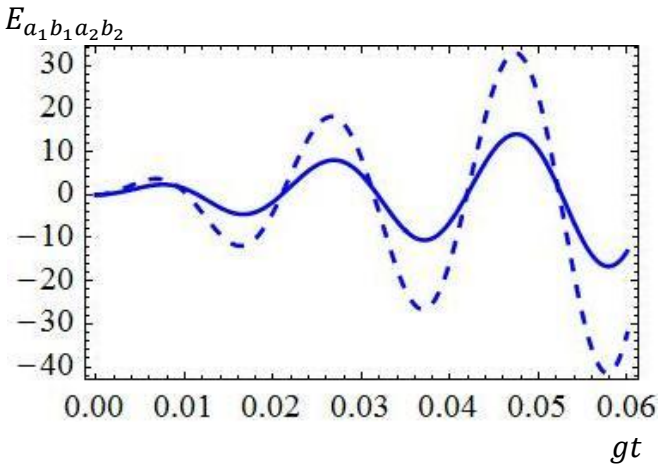

Figure 4.13: Temporal variation of $E_{a_1b_1a_2b_2}$ for phase angle $\theta_1 = \theta_2 = 0$, $g/\omega_m = 0.0033$, $g/\xi = 0.12$ and $|\alpha_k| = 3$, $|\alpha_j| = 3$, $|\beta_k| = 2$, $|\beta_j| = 2$ (solid line) ; $|\alpha_k| = 4$, $|\alpha_j| = 3$, $|\beta_k| = 2$, $|\beta_j| = 1$ (dotted line).

Figure (4.13) displays the temporal variation of equation (4.60) for different weight factor of input state. From this it is clear that the entanglement parameter oscillates between nonclassical to classical regime with gradually increasing the degree. The degree of non-separability increases with photon tunneling strength but remain same for coupling strength. For zero photon tunneling strength there is no signature of entangled

state. This is because when photon tunneling strength is switched off, there is no interaction between the field modes and entangled state is ruled out. Interestingly, the phase variation shows that non-separable state is observed for all possible phase angle. Phase variation of input field mode are summarized in the following tables 4.1 and 4.2 as follows

Inter-mode	Li et al criterion 1												
	$\theta_2 = 0$							$\theta_1 = 0$					
θ_1 or θ_2	0	π /4	π /2	3π /4	π	5π /4	3π /2	π /4	π /2	3π /4	π	5π /4	3π /2
$a_k b_k b_j$	p	p	p	p	np	np	np	np	np	np	np	p	p
$a_k b_j b_k$	p	p	p	p	p	p	p	p	p	p	p	p	p
$a_k a_j b_j$	p	p	p	p	p	p	p	p	p	p	p	p	p
$a_j a_k b_j$	p	p	p	p	p	p	p	p	p	p	p	p	p

Table 4.1: Phase variation of different three mode entanglement factors according to Li et al criterion 1.

Inter-mode	Li et al criterion 2												
	$\theta_2 = 0$							$\theta_1 = 0$					
θ_1 or θ_2	0	π /4	π /2	3π /4	π	5π /4	3π /2	π /4	π /2	3π /4	π	5π /4	3π /2
$a_k b_k b_j$	p	p	p	p	p	p	p	p	p	p	p	p	np
$a_k b_j b_k$	p	np	np	np	p	p	np	p	p	p	p	np	np
$a_k a_j b_j$	np	p	p	p	p	np	np	np	np	np	p	p	p
$a_j a_k b_j$	p	p	p	p	p	np	np	np	np	np	p	p	p
$a_1 b_1 a_2 b_2$	p	p	p	p	p	p	p	p	p	p	p	p	p

p≡ possible , np≡ not possible.

Table 4.2: Phase variation of different three mode entanglement factors according to Li et al criterion 2.

4.6.5 Numerical Solutions

In present section, we numerically solve the system Hamiltonian to account the mechanical damping, cavity losses and also the presence of driving term. The driven-dissipative master equation is given by

$$\dot{\rho} = -i[H, \rho] + L_\rho \tag{4.60}$$

where L_ρ the Lindblad operator and defined by $L_\rho = L_{a_1} + L_{a_2} + L_{b_1} + L_{b_2}$, with

$$L_{a_j}\rho = \frac{\kappa_j}{2}(2a_j\rho {a_j}^\dagger - {a_j}^\dagger a_j\rho - \rho\, {a_j}^\dagger a_j)$$

$$L_{b_j}\rho = \frac{\gamma_j}{2}(n_{th}+1)\left(2b_j\rho {b_j}^\dagger - {b_j}^\dagger b_j\rho - \rho\, {b_j}^\dagger b_j\right) + \frac{\gamma_j}{2}n_{th}\left(2b_j\rho {b_j}^\dagger - {b_j}^\dagger b_j\rho - \rho\, {b_j}^\dagger b_j\right)$$

where κ_j and γ_j are cavity loss rates of the cavity field modes and mechanical damping of the mechanical field modes, respectively ($j = 1,2$). Here, $n_{th} = 1/[\exp\left(\frac{\hbar\omega_m}{k_B T}\right) - 1]$ indicates the thermal phonon number at temperature T.

The system Hamiltonian under RWA takes the form (in presence of driving)

$$H = \Delta_1\, a_1^\dagger a_1 + \Delta_2\, a_2^\dagger a_2 + \omega_m b_1^\dagger b_1 + \omega_m b_2^\dagger b_2 - g a_1^\dagger a_1\left(b_1^\dagger + b_1\right) - g a_2^\dagger a_2\left(b_2^\dagger + b_2\right) - \xi\left(a_1^\dagger a_2 + a_2^\dagger a_1\right) + i\Omega_1\left(a_1^\dagger + a_1\right) + i\Omega_2\left(a_2^\dagger + a_2\right) \tag{4.61}$$

where $\Delta_j = \omega_{cj} - \omega_l$ is the frequency detuning between of the driving laser frequency and cavity frequency. The field amplitude of the driving field is Ω_j, which is expressed in terms of input power P_j and is given by $|\Omega_j| = \sqrt{2P_j k_j / \hbar\omega_l}$.

Without loss of generality and homogeneity, we assume two cavity systems are alike, such that $\Delta_1 = \Delta_2 = \Delta$, $k_1 = k_2 = k$, $\gamma_1 = \gamma_2 = \gamma$ and $\Omega_1 = \Omega_2 = \Omega$.

Figure 4.14 and 4.15 represent the variation of tri-modal entanglement factors $\zeta's$ and $\varepsilon's$ as a function of cavity detuning with different values of photon tunnelling strength for (a) $a_k b_k b_j$ mode (b) $a_k b_j b_k$ mode (c) $a_k a_j b_j$ mode (d) $a_j a_k b_j$ mode, respectively.

The negative values of $\zeta's$ and $\varepsilon's$ give the signature of intermodal entanglement. The variations of entanglement factors with interaction parameters are very similar to the analytical results as discussed in the section 4.6.3.

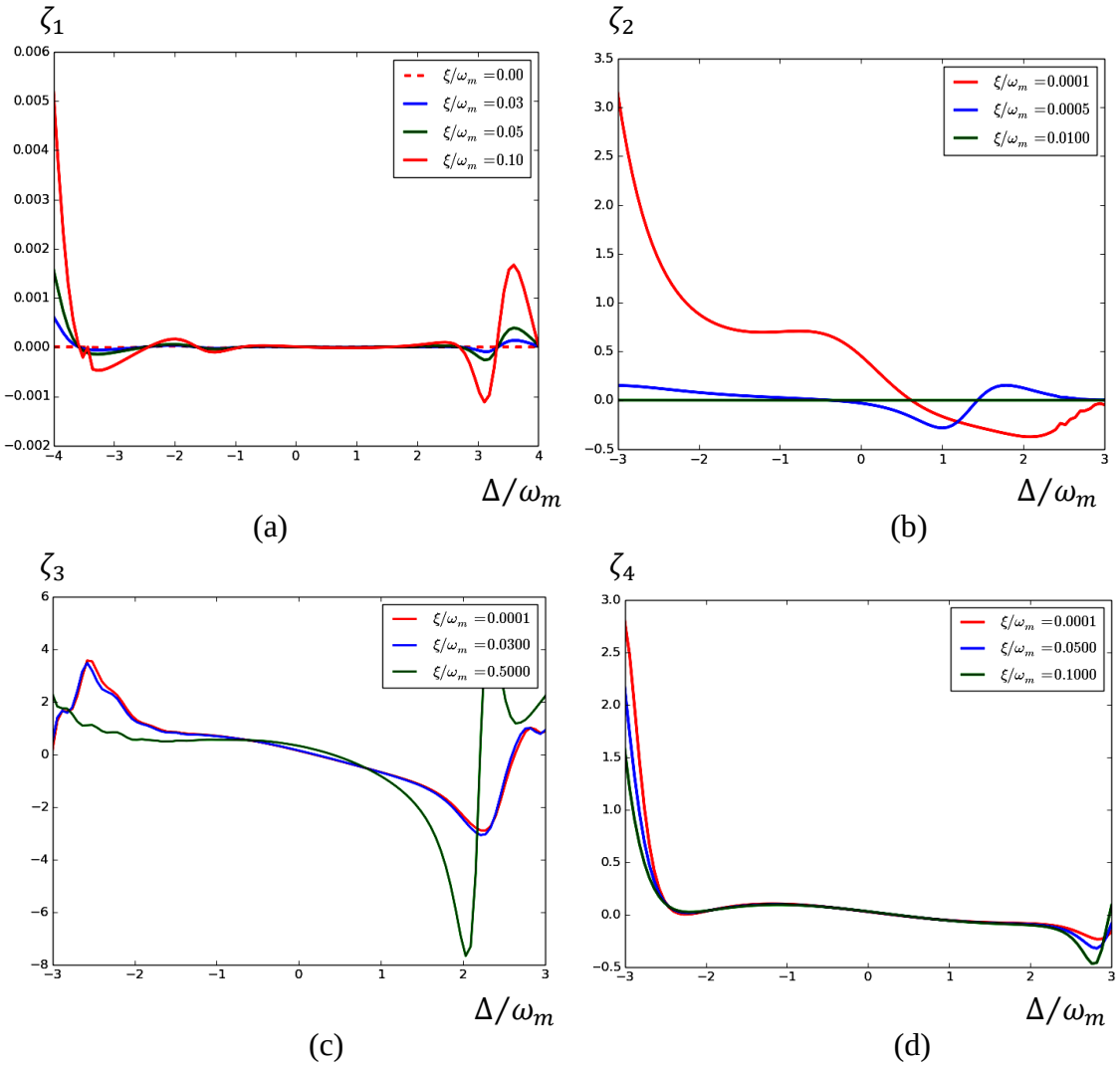

Figure 4.14: Variation of ζ's for three different field modes (a) $a_k b_k b_j$ mode (b) $a_k b_j b_k$ mode (c) $a_k a_j b_j$ mode (d) $a_j a_k b_j$ mode with cavity detuning Δ/ω_m for different values of ξ/ω_m. Other parameters are $g/\omega_m = 0.0033, k/\omega_m = 0.5, \gamma/\omega_m = 10^{-5}$, $\Omega/\omega_m = 0.02$ and $n_{th} = 20$.

The variation of four mode entanglement parameter as a function of cavity detuning with different system parameters is depicted in figure 4.16. The entanglement parameter

$E_{a_1b_1a_2b_2}$ oscillates in between classical to nonclassical region. The fluctuation of $E_{a_1b_1a_2b_2}$ is optimum around resonance condition i.e. $\Delta/\omega_m = 0$. Degree of entanglement gradually decays to zero at the far of Δ/ω_m . From the variation it is clear that when photon tunneling strength increases the degree of non-separability also increases.

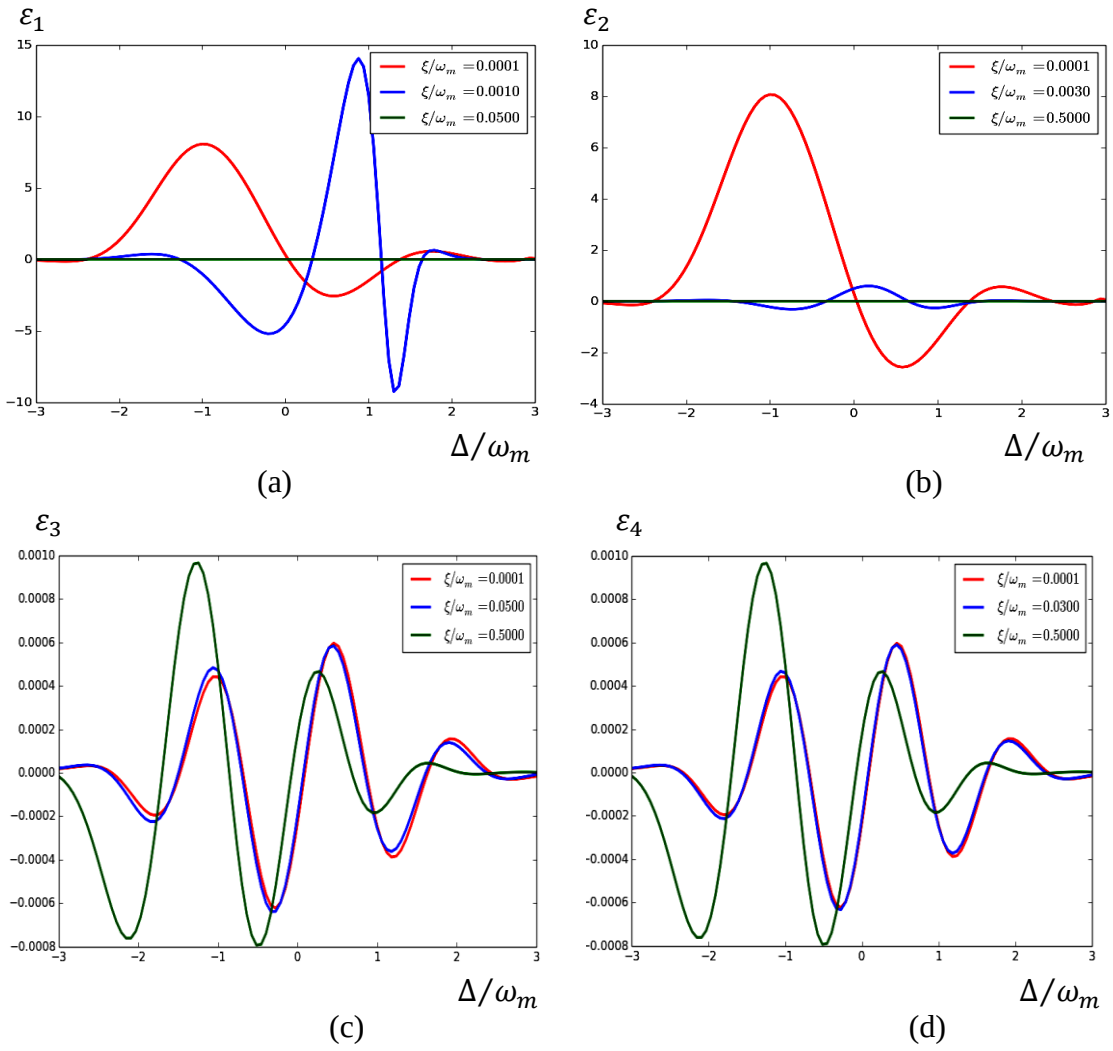

Figure 4.15: Variation of ε's for three different field modes (a) $a_k b_k b_j$ mode (b) $a_k b_j b_k$ mode (c) $a_k a_j b_j$ mode (d) $a_j a_k b_j$ mode with normalized cavity detuning Δ/ω_m for different values of ξ/ω_m. Other parameters are $g/\omega_m = 0.0033, k/\omega_m = 0.5, \gamma/\omega_m = 10^{-5}, \Omega/\omega_m = 0.02$ and $n_{th} = 20$.

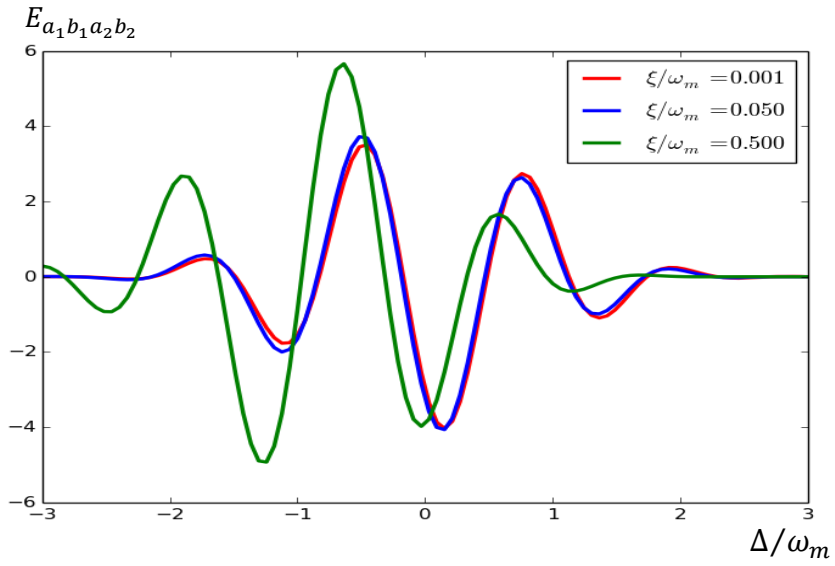

Figure 4.16: Plot of $E_{a_1b_1a_2b_2}$ with normalized cavity detuning Δ/ω_m for different values of ξ/ω_m. Other parameters are $g/\omega_m = 0.0033$, $k/\omega_m = 0.5$, $\gamma/\omega_m = 10^{-5}$, $\Omega/\omega_m = 0.02$ and $n_{th} = 20$.

4.7 Summary

Lower and higher order nonclassicalities for single and compound field mode in two cavity OMS, are rigorously analyzed in the present chapter. The model system is studied here consist of two separated cavities, coupled via photon hopping interaction. We have reported the variation of different nonclassical correlation factors with system parameters, both analytically as well as numerically, for different strengths of photon hopping parameter ξ and coupling term g such that $g < \xi$, $g \approx \xi$ and $g > \xi$.

The squeezing effect is investigated for single mode (cavity field mode and mechanical mode) both in lower and higher order. Lower order study shows that there is no signature of squeezing for both the cavity field mode and mechanical mode. Interestingly, higher order variation shows that amplitude squared squeezing is possible for cavity mode. But amplitude cube squeezing is not possible. Again, mechanical mode shows squeezing effect for all higher order. So, this confirms the possibility of

squeezing effect at macroscopic level via mechanical squeezing. The degree of mechanical squeezing is controlled by coupling strength and order number. From the analysis of compound mode quadrature variation, it is observed that squeezing is possible for intra-cavity photon-phonon mode and inter-cavity photon-phonon mode. For inter-cavity photon-photon and phonon-phonon, squeezing is not possible for compound mode. This study of the squeezing effect may be useful for production of low noise signal.

Particle statistics of the model system for single field mode is studied in lower order via Mandel's Q parameter and in higher order via Lee criteria. Both the investigation confirms that single field mode antibunching is not possible in the present system and these field mode show super-Poissonian statistics. Although single mode antibunching is not possible but intermodal antibunching is possible for intra-cavity photon-phonon mode and inter-cavity photon-phonon mode. The degree of antibunching for intra-cavity field modes is more as compared to inter-cavity field modes. The photon-photon and phonon-phonon intermodal statistics are Poissonian in nature. Higher order study of compound field mode show that intermodal antibunching is observed for intra-cavity field modes, inter-cavity field modes and inter-cavity photon-photon mode. The lower order study shows photon-photon intermodal statistics is Poissonian whereas for higher order the statistics is sub-Poissonian. Higher order study is also revealed that the degree of intermodal antibunching depends on phase of the input state.

Intermodal entanglement in two field mode is studied via both lower and higher order. Lower order study is done by using Duan et al criteria and two Hillery-Zubairy criteria. According to Duan et al criteria intermodal entanglement is possible for intra-cavity photon-phonon mode and inter-cavity photon-phonon field modes. The nonclassical

correlation parameter fluctuates in between nonclassical and classical region. On the other hand both the Hillery-Zubairy criteria show that non-separable state is possible only for intra-cavity field modes both in lower as well as higher order. All the three criteria show that there is no signature of entanglement for inter-cavity field modes and inter-mechanical modes. Tri-modal entangled state is observed for all the possible modes and this analysis is based on Li et al criteria. The possibility of three mode entanglement for different phase of the input state is also reported. The degree of two mode lower order non-separability is more than tri-modal non-separability. The present system consists of four field modes such that there is a possibility of four mode entanglement, which is also investigated by Li et al criteria. The four mode correlation factor oscillates in between entangled (nonclassical) to disentangled (classical) regions. The degree of non-separability for four field modes is more as compared to three modes. As the system is experimentally realizable, this should be useful for generation of multimode entangled state. The phase variation of the field mode is useful for quantum metrology.

All the studies reveal that the degree of nonclassicalities are depended on the optomechanical coupling strength in the cavity and the photon hopping interaction term between the cavities. Higher order study shows that degree of nonclassicalities increases with order number. This study should be useful for detection of nonclassicalities via higher order where degree of nonclassicalitites is enhanced as compared to lower order. This study also reveals that the possibility of generation of nonclassical states at macroscopic or mesoscopic regime and also shows the state transfer from intra-cavity field mode to inter-cavity field mode via photon hopping interaction.